Recent Advances in Experimental Techniques for Flow and Mass Transfer Analyses in Thermal Separation Systems

Uwe Hampel[1,2,*], Markus Schubert[1], Alexander Döß[1], Johanna Sohr[2], Vineet Vishwakarma[1,2], Jens-Uwe Repke[3], Sören J. Gerke[3], Hannes Leuner[3], Matthias Rädle[4], Viktoria Kapoustina[4], Lucas Schmitt[4], Marcus Grünewald[5], Jost H. Brinkmann[5], Dominik Plate[5], Eugeny Y. Kenig[6], Nicole Lutters[6], Lukas Bolenz[6], Felix Buckmann[6], Dominique Toye[7], Wolfgang Arlt[8], Thomas Linder[8], Rainer Hoffmann[9], Harald Klein[10], Sebastian Rehfeldt[10], Thomas Winkler[10], Hans-Jörg Bart[11], Dominic Wirz[11], Jonas Schulz[11], Stephan Scholl[12], Wolfgang Augustin[12], Katharina Jasch[12], Florian Schlüter[12], Natalie Schwerdtfeger[12], Stefan Jahnke[12], Andreas Jupke[13], Christoph Kabatnik[13], Andreas Siegfried Braeuer[14], Mirko D'Auria[14], Thomas Runowski[15], Maria Francisco Casal[15], Karsten Becker[15], Anna-Lena David[15], Andrzej Górak[16], Mirko Skiborowski[16], Kai Groß[16], Hina Qammar[16]

DOI: 10.1002/cite.202000076

Modelling flow and mass transfer of thermal separation equipment constitutes one of the most challenging tasks in fluids process engineering. The difficulty of this task comes from the multiscale multiphase flow phenomena in rather complex geometries. Both analysis of flow and mass transfer on different scales as well as validation of models and simulation results require advanced experimental and measurement techniques. As a follow-up to intensive discussions during the 2019 Tutzing Symposium "Separation Units 4.0" a wide set of available modern experimental technologies is presented.

Keywords: Experimental techniques, Measurement techniques, Thermal separation systems

Received: April 07, 2020; *accepted:* April 08, 2020

[1]Prof. Uwe Hampel, Dr. Markus Schubert, Alexander Döß, Vineet Vishwakarma
u.hampel@hzdr.de
Helmholtz-Zentrum Dresden-Rossendorf, Institut für Fluiddynamik, Bautzner Landstraße 400, 01328 Dresden, Germany.

[2]Prof. Uwe Hampel, Johanna Sohr, Vineet Vishwakarma
Technische Universität Dresden, Institut für Energietechnik, 01062 Dresden, Germany.

[3]Prof. Jens-Uwe Repke, Sören J. Gerke, Hannes Leuner
Technische Universität Berlin, Institut für Prozess- und Verfahrenstechnik, Straße des 17. Juni 135, 10623 Berlin, Germany.

[4]Prof. Matthias Rädle, Dr. Viktoria Kapoustina, Lucas Schmitt
Hochschule Mannheim, Center for Mass Spectrometry and Optical Spectroscopy, John-Deere-Straße 81A, 68163 Mannheim, Germany.

[5]Prof. Marcus Grünewald, Jost H. Brinkmann, Dominik Plate
Ruhr-Universität Bochum, Lehrstuhl für Fluidverfahrenstechnik, Universitätsstraße 150, 44801 Bochum, Germany.

[6]Prof. Eugeny Y. Kenig, Dr. Nicole Lutters, Lukas Bolenz, Felix Buckmann
Universität Paderborn, Fakultät für Maschinenbau, Lehrstuhl für Fluidverfahrenstechnik, Pohlweg 55, 33098 Paderborn, Germany.

[7]Prof. Dominique Toye
Universite de Liège, Department of Chemical Engineering, Allée du six Août, 17B, 4000 Liège 1, Belgium.

[8]Prof. Wolfgang Arlt, Thomas Linder
Friedrich-Alexander-Universität Erlangen-Nürnberg, Institute of Separation Science and Technology, Egerlandstraße 3, 91058 Erlangen, Germany.

[9]Dr. Rainer Hoffmann
Linde Aktiengesellschaft, Engineering Division, Dr.-Carl-von-Linde-Straße 6–14, 82049 Pullach bei München, Germany.

[10]Prof. Harald Klein, Dr. Sebastian Rehfeldt, Thomas Winkler
Technical University of Munich, Department of Mechanical Engineering, Institute of Plant and Process Technology, Boltzmannstraße 15, 85748 Garching, Germany.

[11]Prof. Hans-Jörg Bart, Dominic Wirz, Jonas Schulz
Technische Universität Kaiserslautern, Lehrstuhl für Thermische Verfahrenstechnik, PF 3049, 67653 Kaiserslautern, Germany.

[12]Prof. Stephan Scholl, Dr. Wolfgang Augustin, Dr. Katharina Jasch, Florian Schlüter, Natalie Schwerdtfeger, Stefan Jahnke
Technische Universität Braunschweig, Institute for Chemical and Thermal Process Engineering, Langer Kamp 7, 38106 Braunschweig, Germany.

[13]Prof. Andreas Jupke, Christoph Kabatnik
RWTH Aachen University, Aachener Verfahrenstechnik, Fluidverfahrenstechnik, Forckenbeckstraße 51, 52074 Aachen, Germany.

1 Introduction

Fluid separation processes are antetypes of multiscale multiphase processes. Their functional principles base on the transfer of a species from one into another thermodynamic phase following a thermodynamic gradient, given, e.g., by volatility or solubility [1]. Efficiency of such processes is bound to large contact areas between the phases as well as enhanced convective transport near their interfaces. Consequently, enormous effort is being spent to design process devices and internals, which provide large mass transfer areas and intensified convective transport. Recent years have seen remarkable developments in new structured and unstructured packings [2], trays with integrated flow guides [3], efficient droplet separators, internals for extractors and new concepts of process intensification, such as HiGEE machines [4], reactive distillation and others. Beside optimization of mass transfer other important research and development directions in modern thermal separation technology are overall energy efficiency, prevention of fouling and foaming, flexible operation, new in situ measurement techniques, and handling of complex fluids, such as azeotropes and fluids of high viscosity or very low surface tension.

Key aspects of modern separation technology are modelling and simulation. The multiscale multiphase nature of the problem turns this into a very difficult endeavour. Modelling strategies today typically try to couple simulation schemes at different scales, starting from molecular dynamics simulations for the thermodynamics of mass transfer, direct numerical simulations to resolve boundary layers and mass transfer across interfaces, and eventually multiphase CFD and lumped-parameter models on the device scale [1]. For all the scales, experimental data are needed. Such data are obtained from experiments in laboratory and technical-scale test facilities. Moreover, in recent years many new measurement techniques have been made available for such studies. Most notable are measurement techniques with very high spatial and temporal resolution for the validation of CFD codes and tomographic measurement techniques, which give insight into opaque systems. Data from the micrometer and millimeter scale can today be obtained with novel laser-based and optical measurement techniques. Such are for example micro-PIV and fluorescence techniques. For the larger scale, tomography techniques, reaching from wire-mesh sensors and gamma ray tomography for large columns, to high-resolution X-ray tomography and dynamic ultrafast X-ray tomography [5], are available.

The participants of the 2019 Tutzing Symposium "Separation Units 4.0" vividly discussed existing technologies and future trends of experimental investigations of separation systems with the purpose to improve understanding and modelling of multiscale multiphase transport processes. The following chapters present a summary of the existing techniques and infrastructures with a focus on German academic and industrial laboratories, owing to the nature of this event. For an appropriate structuring of the article, we divide the techniques into such for (1) packings, (2) for full columns, trays, and feed pipes, (3) for evaporators and condensers, for (4) liquid-liquid extraction and (5) for intensified separation technologies. For each of these techniques, the corresponding research groups are given in the subchapter headlines.

2 Experimental Techniques for Packings

2.1 Imaging Techniques for the Investigation of Liquid Film Flow over Packing Surfaces (TU Berlin, Hochschule Mannheim)

The geometric features of packing elements significantly impact the separation performance of distillation and absorption towers by increasing the wettability and intensifying the interaction of liquid and gas flow. However, the underlying phenomena induced by textured packing materials are not fully understood and demand high-resolution experimental and numerical methods.

Advances in optical measurement technologies now enable highly detailed non-invasive analysis of mass and momentum transport phenomena in thin liquid films. The local influence of the packing surface geometry on momentum transfer inside liquid film flow is analysed with particle image velocimetry (PIV) by measuring statistical relevant snapshots of the flow field enabling for the detection of detaching eddies or recirculating flow regions and particle tracking velocimetry (PTV) to additionally determine individual particle path and residence times. To study the effect of micro- and macro-structures of structured packing, Gerke and Repke [6] applied a stereoscopic PIV to liquid film flow over transparent mouldings with refractive index matching. This approach allows to record the flow field through the solid plate elements from several perspectives

[14]Prof. Andreas Siegfried Braeuer, Mirko D'Auria
Technische Universität Bergakademie Freiberg (TUBAF), Institute of Thermal-, Environmental and Resources' Process Engineering (ITUN), Leipziger Straße 28, 09599 Freiberg, Germany.

[15]Dr. Thomas Runowski, Maria Francisco Casal, Dr. Karsten Becker, Anna-Lena David
Bayer AG, Engineering & Technology, Thermal Separation Technologies, 51368 Leverkusen, Germany.

[16]Prof. Andrzej Górak, Dr. Mirko Skiborowski, Kai Groß, Hina Qammar
TU Dortmund University, Department of Biochemical and Chemical Engineering, Laboratory of Fluid Separations, Emil-Figge-Straße 70, 44227 Dortmund, Germany.

independent of the surface texture and waves. The liquid film is seeded with micro-metre sized solid particles, which passively follow the flow. A pulsed laser light sheet illuminates the particles and images are recorded from two perspectives at defined time-steps. The statistical particle displacement between the consecutive recordings is computed using cross-correlation methods and the spatial transformation from a volumetric calibration resulting in a 2D3C flow field. Thus, the pseudo stationary volumetric flow field can be captured by successive light sheet scanning.

Kapoustina et al. [7] accomplished oxygen concentration field measurements inside the liquid film over a single micro-structure using planar light-induced fluorescence (PLIF). The micro-metre resolution allows to capture concentration boundary layer profiles and thus analysis of local mass transfer coefficients. To get a direct measurement of oxygen concentrations, small amounts of the fluorescence indicator based on a ruthenium-complex are homogenously dissolved in the liquid and excited by a planar laser light sheet. The recorded fluorescence light intensity is inversely proportional to the oxygen concentration because the fluorescence is quenched in the presence of dissolved oxygen. These measurements are straightforwardly extendible to volumetric measurements by light-sheet scanning and high-speed imaging to capture dynamic effects. The integration of PLIF into the SPIV setup allow simultaneous mass and momentum transfer measurements and extends the PLIF setup to textured surfaces and wavy flow (Fig. 1).

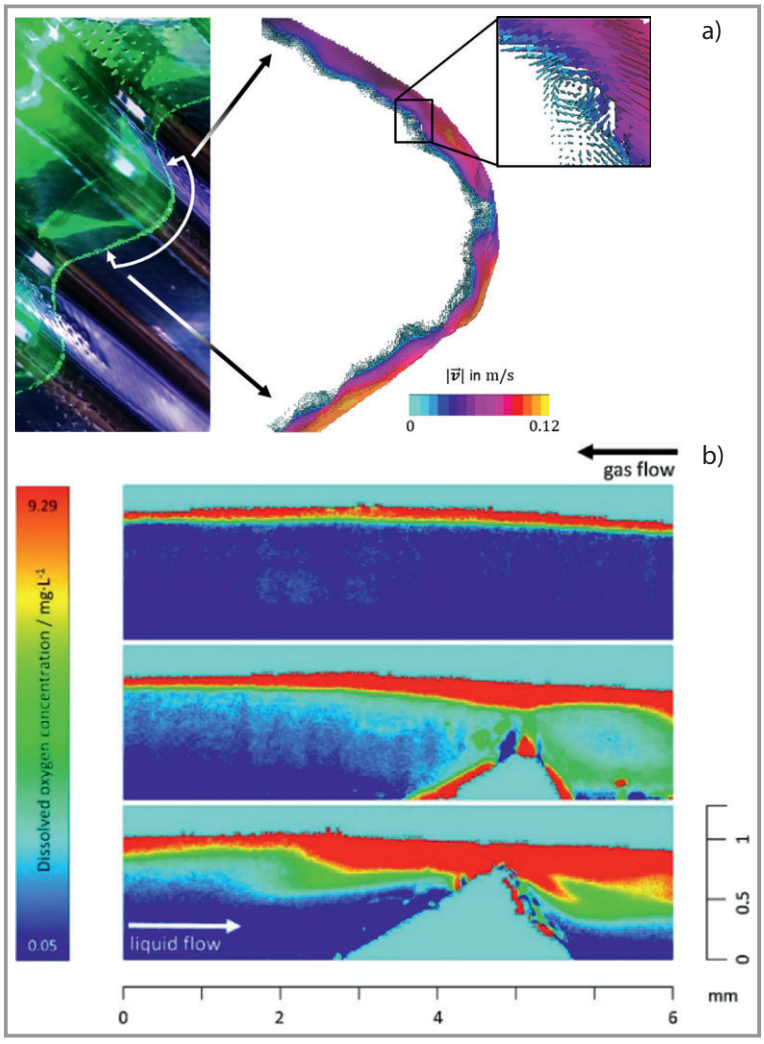

Figure 1. Optical measurements in liquid film flow: a) velocity field over open structured packing obtained with SPIV. b) Concentration fields over a single micro-structure obtained with PLIF.

The presented methods and studies contribute to the development of separation apparatuses and the development of innovative design methods like miniaturized representative experimental setups. These smaller scale experiments are crucial to get an even better understanding of the underlying flow phenomena and provide fundamental data for the validation of more detailed modelling and CFD simulations. In the future, these approaches will be coupled with optimal design using CFD and 3D printing for the engineering and manufacturing of innovative specifically enhanced packing geometries.

2.2 Miniaturized Measurement Cells for Flow and Mass Transfer Studies (TU Berlin, Ruhr-Universität Bochum)

The development of miniaturized experimental set-ups originates from the idea to reduce the dimensions of the experimental set-ups to a minimum required size that allows representative measurements of fluid dynamic and mass transfer characteristics of columns with structured packings as predominant in industrial sized columns [8]. Especially the periodic geometry of structured packings is suitable for reducing the complexity to a small section of the packing and to investigate all necessary parameters for column design in a miniaturized experimental set-up.

In recent investigations, miniaturized experimental set-ups were built to investigate the influence of the number of packing sheets (Ruhr-University Bochum) or the influence of the geometry of the packing sheet (Technical University of Berlin) to find the minimum required and smallest possible dimension for such a miniaturized experimental set-up [9]. Within the miniaturized experimental set-ups (Fig. 2), fluid dynamic parameters like liquid hold-up, film thickness and gas pressure loss were measured to analyze the connection between a miniaturized set-up to a structured packing column.

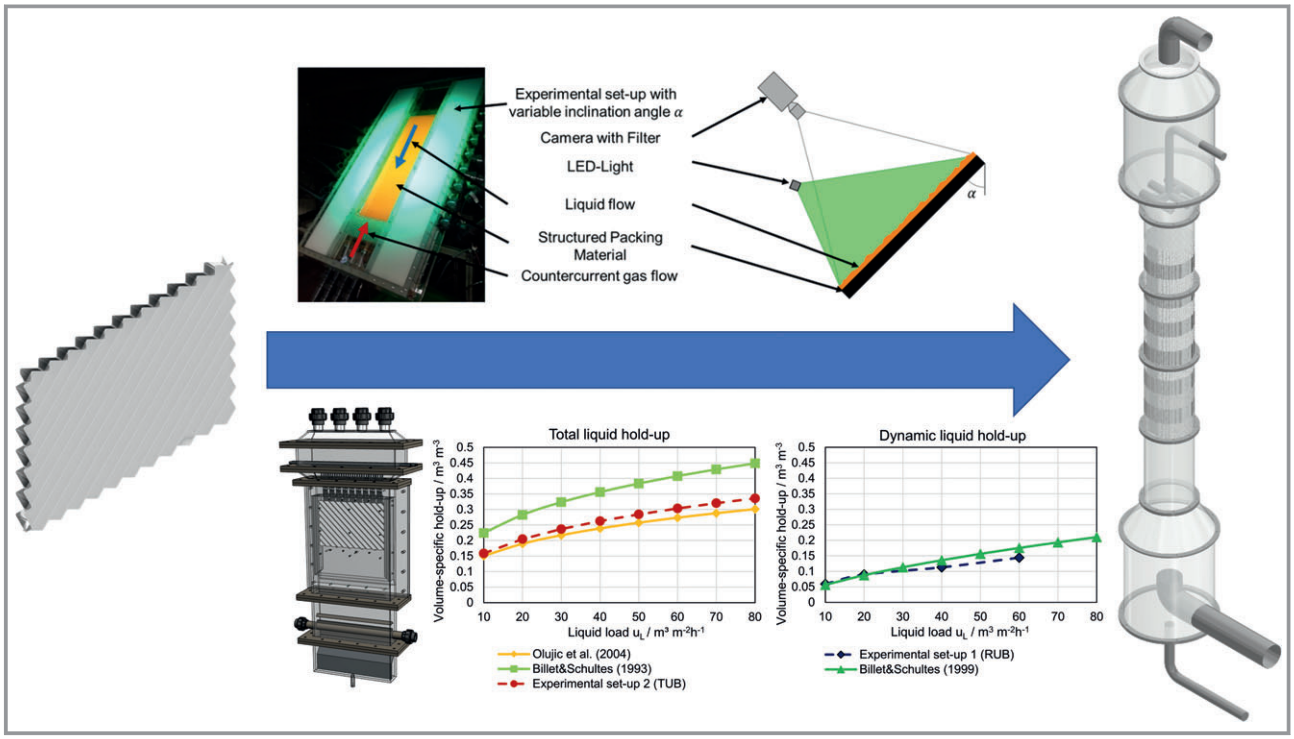

Figure 2. Miniaturized experimental setup to investigate the geometry of packing sheets with the Light-induced Fluorescence Method (top) and miniaturized experimental setup to investigate the influence of the number of packings sheets with the draining method (bottom).

However, other characteristic values for fluid dynamics and mass transfer can be further determined using either state of the art sensors for process performance values like gas and liquid concentrations or advanced optical measurements technologies like (planar-)light induced fluorescence (P-LIF), structured light scanning (SLS), PIV, and PTV as well as advanced flow imaging technology like wire-mesh sensors (WMS) and X-ray tomography to gain further insights of the two-phase flow in structured packings.

The outcome of these experimental investigations can be further applied to advanced three-dimensional column models to accurately and cost-effectively predict the performance of a column [9]. These three-dimensional columns models are especially advantageous compared to today's state of the art plug flow models that usually do not take small- and large-scale maldistributions of the two-phase flow into account and comprise therefore remarkable uncertainties. Besides the more detailed modelling, this approach allows investigations of the real process fluid mixtures on the intentionally chosen packing material even at a very early stage of the design of a column, which can further lead into remarkable time savings [8].

2.3 Investigation of the Liquid Flow Morphology in Structured Packings Using High-Resolution X-ray Tomography (Paderborn University, University of Liège)

Gas-liquid separation processes with a viscous liquid phase, e.g., the removal of monomers from a polymer solution, are of high relevance for the chemical industry. However, standard modelling approaches fail to predict the separation efficiency, since required mass transfer correlations are obtained for low-viscosity test mixtures and have limited validity for more viscous liquids. The hydrodynamic analogies (HA) approach evolving at Paderborn University does not rely on empirical mass transfer correlations. Instead, information on dominating flow patterns within column units is essential. The HA approach is a promising alternative for the prediction of separation efficiency for viscous systems, especially in packed columns, provided that the flow patterns inside packings are identified. While for low viscosity, an analogy with uniform film flow on the packing surface can be applied, the flow morphology becomes more complex for systems with increased viscosity.

The flow patterns for various liquids and packing geometries have been investigated by high-energy X-ray tomography using the facilities and methodology developed by the University of Liège [10] (Fig. 3a). A packed column with a diameter of 100 mm operated continuously with counter-

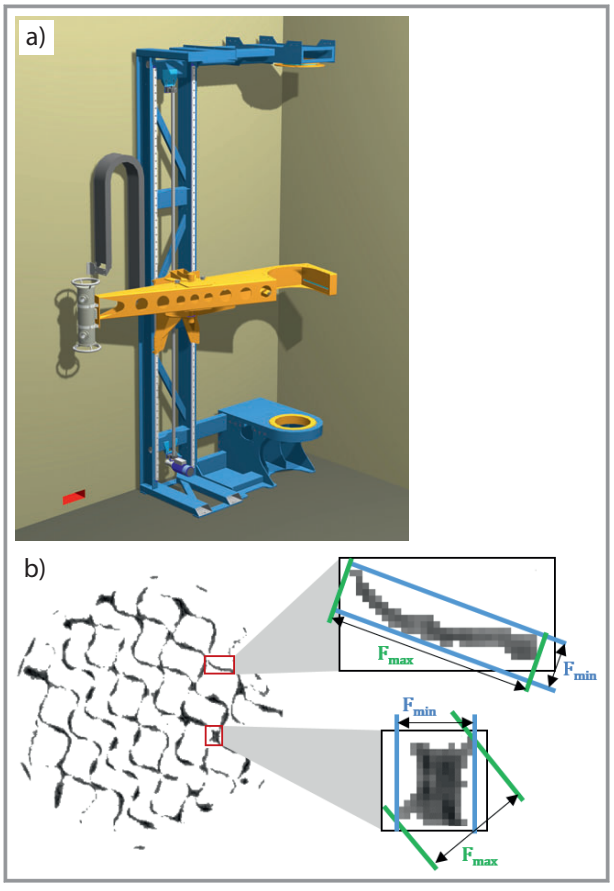

Figure 3. a) High-resolution X-ray tomograph at Université de Liège. b) Cross-sectional image of the liquid distribution inside a structured packing. Film flow and C-P liquid are distinguished by the maximum and minimum Feret diameter of the pixel structure. The data is needed for HA models developed at Paderborn University.

currently flowing liquid and air has been scanned by X-ray tomography. The projection data are converted to cross-sectional images of the liquid distribution with a spatial resolution of $0.36 \times 0.36\,mm^2$. Proper modelling and interpretation of tomographic data are an important prerequisite for their accurate application within the HA approach. As shown in Fig. 3b, film flow is the dominating pattern in the structured packing. It can easily be identified, since it follows the shape of the corrugated sheets. Additionally, contact-point (C-P) liquid representing liquid accumulated at the contact points of adjacent packing sheets can be observed. A particular method was developed to assign each pixel structure in the tomographic images to a certain flow pattern by means of the Feret diameter F [11]. The latter is a distance between two parallel tangents of the pixel structure. For film flow, which appears with a narrow and elongated structure, the ratio F_{max}/F_{min} of the maximum and minimum Feret diameter is considerable. Instead, C-P liquid has a rather compact structure and F_{max}/F_{min} is close to unity. Analysis of the hold-up fractions of different flow patterns shows that for high viscosity, the film flow fraction can drop below 60 %.

Recent work [12] focuses on an improved representation of the cross-sectional images, aiming to overcome the restriction of limited image resolution and to obtain information about local fluid dynamic parameters such as liquid film thickness and degree of wetting of the packing surface. For this purpose, use is made of a specific characteristic of the tomographic images. All pixels representing the liquid phase appear grey and the brightness of the grey shade corresponds to the area fraction occupied by liquid in the respective pixel. With this information, it is possible to reconstruct the gas-liquid interface by the piecewise linear interface calculation method, which has already found application in multiphase flow simulations.

2.4 Investigation of Two- and Three-Phase Flow in Packings with High-Resolution X-ray Tomography (Friedrich-Alexander-Universität Erlangen-Nürnberg)

The X-ray computed tomograph available at the Institute of Separation Science and Technology in Erlangen allows scanning of packings and other equipment at a very high spatial resolution down to 80 µm. The used third generation X-ray CT scanner is custom-designed for process engineering applications and has been developed by the Fraunhofer Development Center for X-ray Technology in Fürth. Further information on the X-ray CT scanner and the distillation measurements are given in Schug and Arlt [13]. Fig. 4 shows the typical procedure from the measurement up to the results. The X-ray source and detector rotate around the vertical axis and are height-adjustable, enabling the investigation of the flow in a column without influencing it. This provides a wide range of application. While distillation has been object of fluid dynamic investigations already for several decades, other unit operations such as adsorption, extraction and reaction gain importance lately [14]. Hereafter, three-phase distillation is exemplary picked out to explain the opportunities and limitations of this measuring device. The main limitation is the selection of a suitable three-phase system, because it has to be possible to distinguish all phases on the CT images. Water/1,2-Dichlorobenzene(DCB)/air on aluminium packings meet this criterion, but for a quantitative evaluation an image post-processing is necessary, which assigns every pixel to one phase. Fig. 4 shows different fluid dynamic parameters, some of them are inaccessible with other measuring techniques. The high spatial resolution does not only allow a precise determination of these quantities, but also an identification of the main flow pattern and an analysis of the axial and radial maldistribution of these fluid dynamic parameters (Fig. 4, middle and right). In combination with novel tracer-measurements, which enable the determination of local residence times, it is achievable to create new fluid dynamic

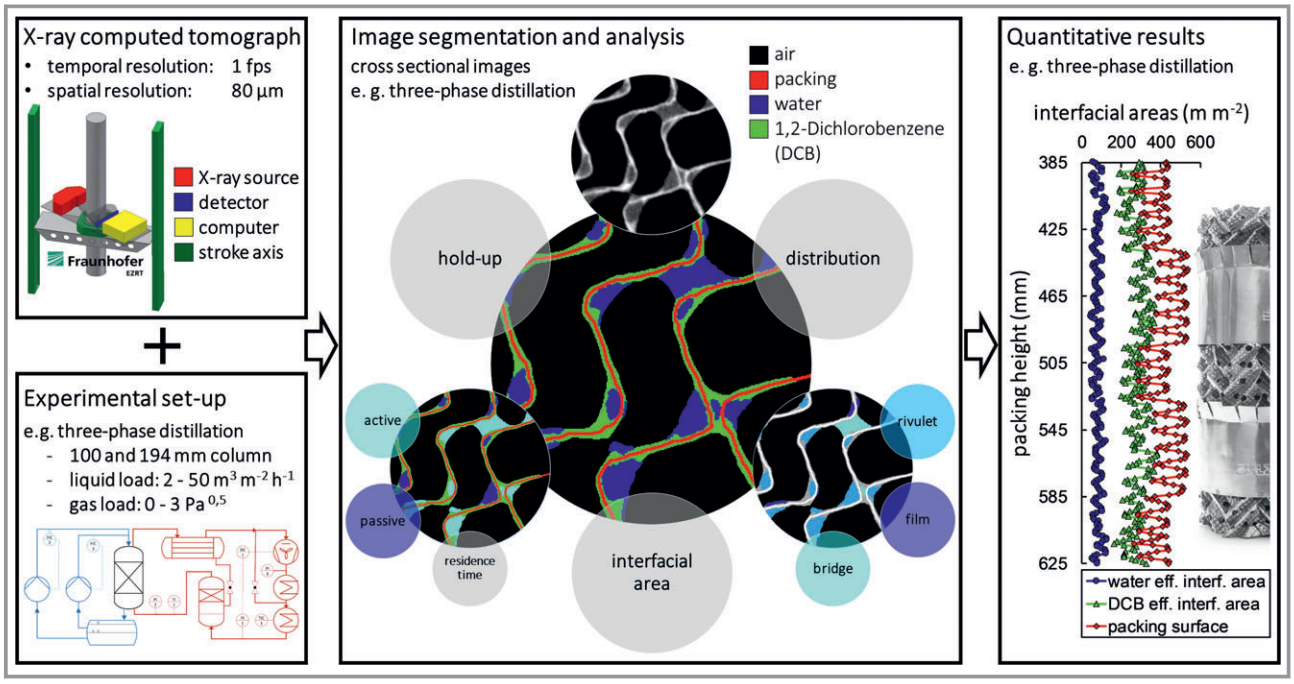

Figure 4. Procedure for X-ray computed tomography in three-phase distillation. CT scan and experimental setup (left), followed by image segmentation and analysis (middle), and analysis of, e.g., interfacial area over packing height (right).

parameters with increased significance. In the field of three-phase distillation, it is therefore possible to explain the frequently occurring mass transfer drops and the limited operating range.

2.5 Dynamic Flow Imaging in Packings with Ultrafast X-ray Tomography (Helmholtz-Zentrum Dresden-Rossendorf)

Amongst others, sandwich packings are an example of a mass transfer intensification technology for distillation columns. They consist of alternating layers of structured packings, one with a higher (holdup layer) and one with a lower specific surface area (de-entrainment layer). Preferentially, such packings are operated between the flooding points of both layers, which results in zones of froth regime and liquid film flow in each sandwich element. Knowledge on liquid holdup dynamics over the entire operating range up to the flooding point is essential for the design of such packings as well as for the development of rigorous efficiency models. The full dynamics of two-phase flow in such packings can be disclosed with ultrafast X-ray computed tomography (UFXCT), which is available at Helmholtz-Zentrum Dresden-Rossendorf [15]. Fig. 5 shows the UFXCT setup and working principle. Within the scanner an electron beam is produced by a high power electron gun and focused on an X-ray target that surrounds the column. The electron beam is swept across the target on a circular path by means of an electromagnetic deflection system. The X-ray radiation traversing the object of investigation is recorded by fast X-ray detectors and from that tomographic images are reconstructed. The scanning speed is up to 8000 cross-sectional images per second with a spatial resolution of about 1 mm [16].

Fig. 5 further shows snap-shots of vertical and cross-sectional liquid holdup distributions in the different layers of a sandwich packing. One can clearly distinguish film and froth flow regimes. Film flow is characterized by low liquid holdup being located on the packing surface only, while channels between sheets are occasionally filled with liquid at froth flow. The height of the evolving froth regime within the de-entrainment layer can be determined from axial scans. The time-resolved plots in Fig. 5 reveal intensive fluctuations of the cross-sectionally averaged liquid holdup within the froth in both layers compared to calm film flow. These intensive fluctuations with time-scales of a few milliseconds are accompanied by frequent renewals of gas-liquid interfaces and cause increased mass transfer rates and improved separation efficiency. The interfacial area density within this dynamic froth flow is also determined from the UFXCT data (Fig. 5). The studies reveal that the interfacial area density in the range of froth flow depends on the specific surface area of the packing regardless of the gas load.

2.6 Study of Mass Transfer in Packing with CO_2 Absorption/Desorption (Paderborn University)

Carbon capture from industrial point sources is a very relevant topic with respect to reduction of greenhouse gas

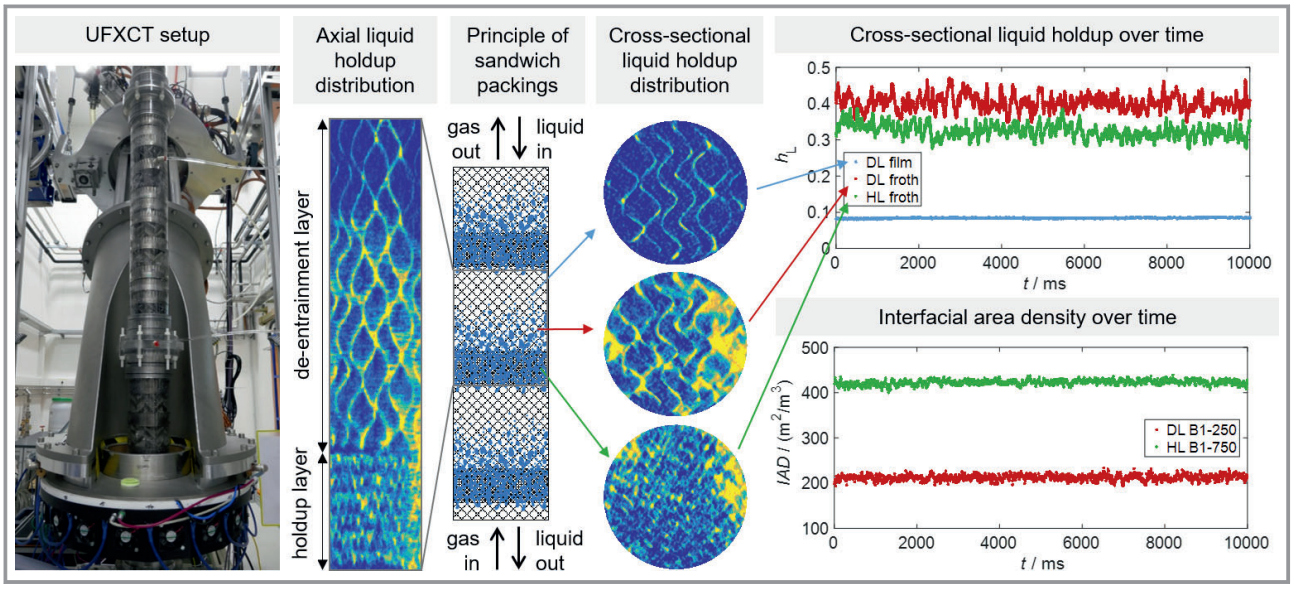

Figure 5. Ultrafast X-ray tomography scanner and exemplary vertical and cross-sectional liquid holdup distributions in a sandwich packing, from which holdup and interfacial area density profiles have been extracted.

emissions. CO_2 capture is typically realized by a closed loop comprising an absorption and a desorption column and based on aqueous solvents. At Paderborn University, a pilot plant [17] is available to investigate new and innovative solvents and column internals for CO_2 absorption. The pilot plant (Fig. 6a) is designed as a multi-purpose and flexible setup. It consists of two glass columns (inner diameter of 0.1 and 0.3 m), while the smaller column is used for absorption and the larger column for desorption or fluid dynamic studies. Experiments can be carried out in different operation modes, namely, in the absorption, desorption and in the closed loop mode. Furthermore, fluid dynamic analyses can be performed.

A particular feature of the plant is that full axial profile data can be obtained, i.e., temperature and both liquid-phase and gas-phase CO_2 concentration profiles. This is essential for the capturing of nonlinear absorption/desorption phenomena in the columns. Samples are taken with the aid of specially developed sampling flanges (Fig. 6b) placed at 0.5 m intervals along the packing height. These flanges are installed between two glass sections, and each flange has two boreholes to insert devices for liquid and gas sample

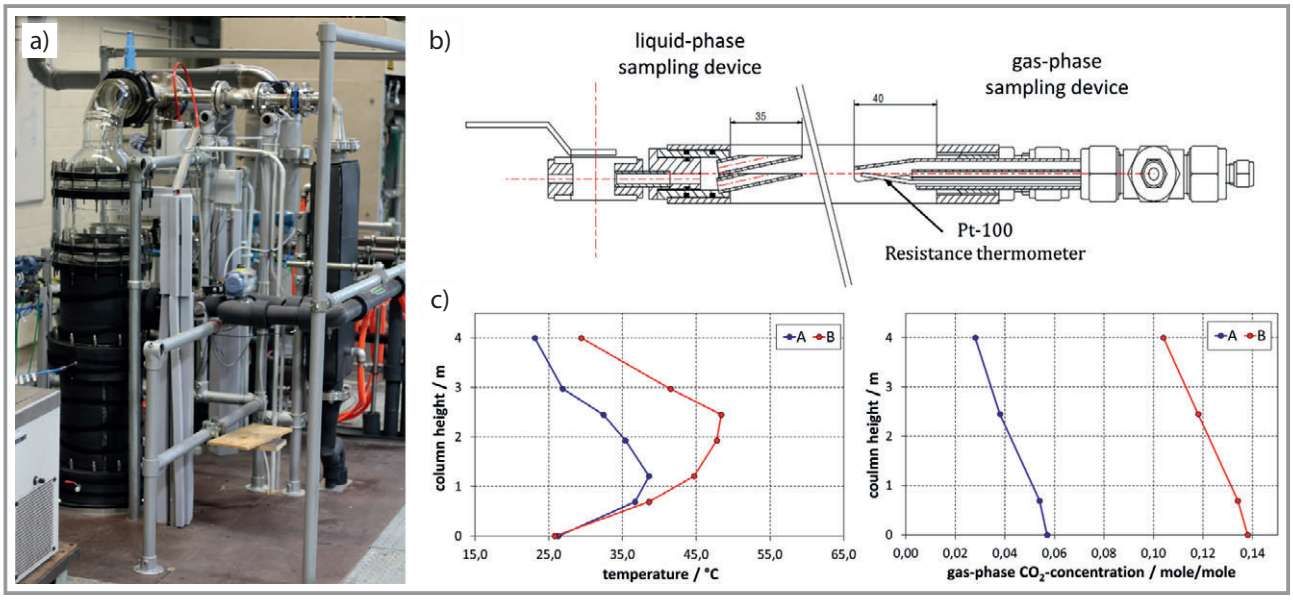

Figure 6. a) Photo of the upper part of the CO_2 absorption/desorption pilot plant at Paderborn University. b) Drawing of the flange with the liquid-phase and gas-phase sampling devices. c) Exemplary gas-phase temperature and CO_2 concentration profiles.

taking. The liquid trickles into the upper tube at the tip of the device, flows through the chamber and trickles out of the lower tube. Thus, liquid holdup in the chamber is always renewed. With a syringe, the liquid can be taken from the chamber and analyzed offline. For gas-phase sampling, a tube is inserted into the flange. This tube is connected to a gas chromatograph via a system of heated pipes and a vacuum pump, so that the gas phase CO_2 concentration can be analyzed online. A Pt100 resistance thermometer is inserted into the tube to measure the temperature at each sampling point. Examples of gas-phase temperature and CO_2 concentration profiles obtained for the system CO_2/aqueous monoethanolamine are shown in Fig. 6c. Experimental results from the pilot plant are used to test new solvents or column internals to evaluate whether they are competitive and to validate process models for further simulations for industrial-scale CO_2 capture [18].

3 Experimental Techniques for Large Columns, Trays, and Feed Pipes

3.1 Liquid Distribution Analysis in Columns with an ATEX Proven Gamma Ray Tomograph (Linde AG)

Gamma ray tomography is a tomographic imaging method of choice for large process equipment. At Linde such a setup is operated at a facility that is run with iso-hexane and nitrogen as fluids as their fluid properties at room temperature are comparable to liquid air components at cryogenic condition [19]. Since a leakage of iso-hexane could create an explosive atmosphere, the whole setup was designed according to ATEX regulations. All non-ATEX-proof components are placed inside a purged Plexiglas housing (Fig. 7a) so that the tomograph can be safely operated inside an ATEX zone. A Cs-137 isotope inside a collimated source container creates a pencil beam detected by an opposite CsI(TI) scintillation detector. The source-detector pair can be moved horizontally, vertically and rotated around the test object using suitable actuators. This gives the projection data that is required for subsequent tomographic image reconstruction. The reconstruction of this data into cross-sectional images of the column is done with standard tomography algorithms. The maximum test object size is Ø 750 mm, the obtainable resolution about 4 mm.

To determine liquid distribution within a static object the ratio of the measured data with liquid flow to the equivalent data for a dry object is used. Fig. 7b, shows an exemplary liquid distribution in a 440 mm column. The tomograph data can be used for optimization of liquid distributor geometry. Other research topics include the investigation of the effect of packing inaccuracies on liquid maldistribution. These results can then be used to define quality limits during packed column production.

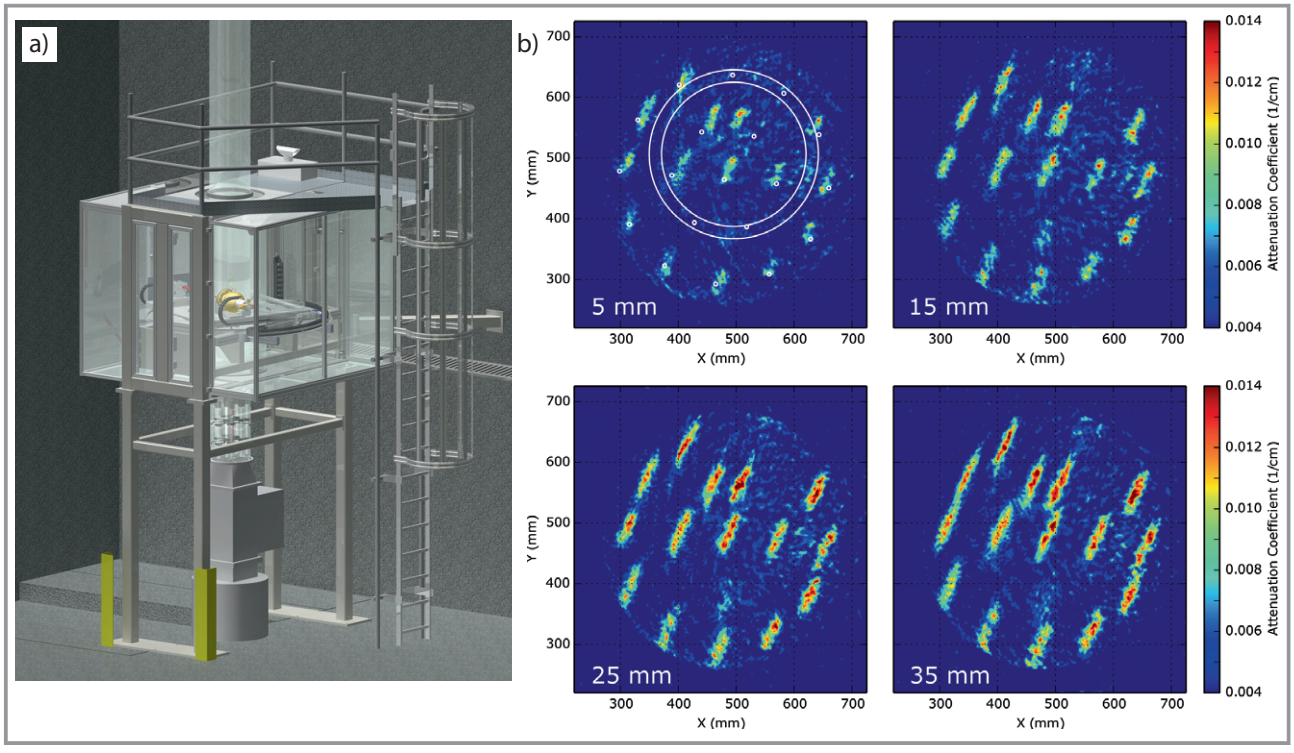

Figure 7. a) View of the pilot plant with gamma ray scanner at Linde Pullach. b) Exemplary images of liquid distribution in a packing (right).

3.2 Investigation of Phase Distribution in Packed Columns (Ruhr-Universität Bochum)

The optimal design of packed columns for resource efficient absorption and distillation processes is of crucial interest for the chemical industry. To date column design is still based on the assumption of superficial velocities for the gas and liquid phase flow. Despite this, maldistribution especially of the liquid phase is a well-known phenomenon. Therefore, the combination of non-ideal operation behavior and its theoretical analysis based on ideal flow patterns results in an unconfident design basis.

An experimental approach to determine radial maldistribution in packed columns based on a wire-mesh sensor has been established at Ruhr-University Bochum [20]. It is complementary to the thermal measurement approach by TU Munich described later (Fig. 8a). The wire-mesh sensor directly measures the liquid and tracer concentration distribution below packings. An integral characterization of the phase distribution below the packing is possible by measuring the change in capacitance caused by liquid flowing through the sensor. Changes in liquid conductivity can be measured and applied to determine the internal mixing of the liquid within the packing using tracer solutions such as sodium chloride (Fig. 8b). Both techniques offer the possibility to set up parameters of advanced column models for absorption and distillation processes considering non-ideal phase distributions.

3.3 Investigation of Two-Phase Flow on Column Trays (Helmholtz-Zentrum Dresden-Rossendorf)

For modelling and improvement of column tray efficiency, knowledge about the two-phase flow including distribution of holdup, clear liquid height and residence time on industrial-scale cross-flow trays is required [21]. For this purpose, researchers at Helmholtz-Zentrum Dresden-Rossendorf developed a novel conductivity-based sensor array for flow studies (Fig. 9a) [22]. It is installed above a test tray with 13.6 % fractional free area inside a DN 800 column mockup as shown in Fig. 9b. Air and water are used as working fluids for the column operation. The sensor array comprises of 776 electrodes that are uniformly distributed over the tray deck with a spatial resolution of 21 mm × 24 mm. During column operation, the sensor obtains holdup profiles for liquid and gas and concentrations of ionic tracer at a very high acquisition rate of 5000 frames per second. Multiple axial measurements at each elevation give a full 3D view of the tray cross-flow. Fig. 9b shows such profiles for elevations up to 80 mm for tray loadings of 3 m^3h^{-1} (water) and 1.6 $Pa^{0.5}$ (air). In this example, low liquid fraction in the froth due to jet formation and weeping as well as higher liquid holdup in the upper planes resulting from reduced air pressure and jet breakup can be observed. Statistical analysis of the sensor data in the spray zone allows the determination of the froth height, which can otherwise only be estimated from visual observation. The occurrence of higher gas holdup near the tray deck also questions the clear liquid height measurement based on manometer data. Integrating the holdup data at each probe up to the froth height

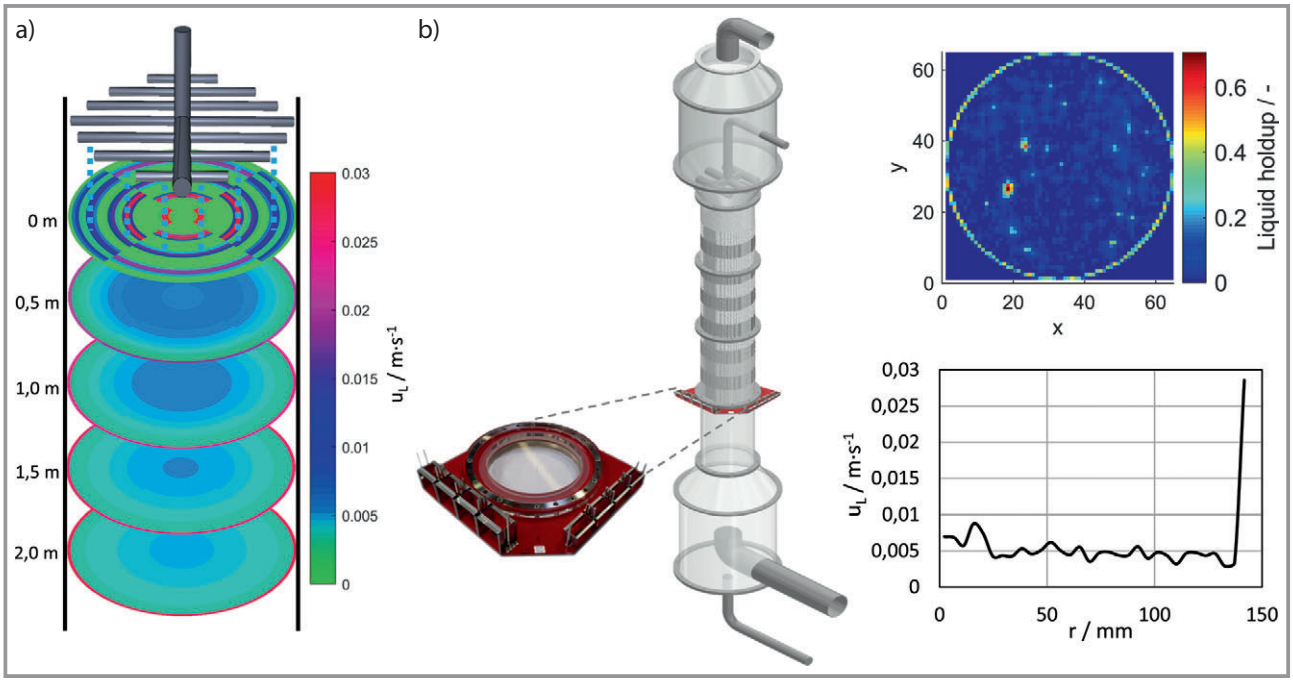

Figure 8. a) Liquid maldistribution in a randomly packed column. b) Application of the wire-mesh sensor for the determination of radial phase distribution in packed columns.

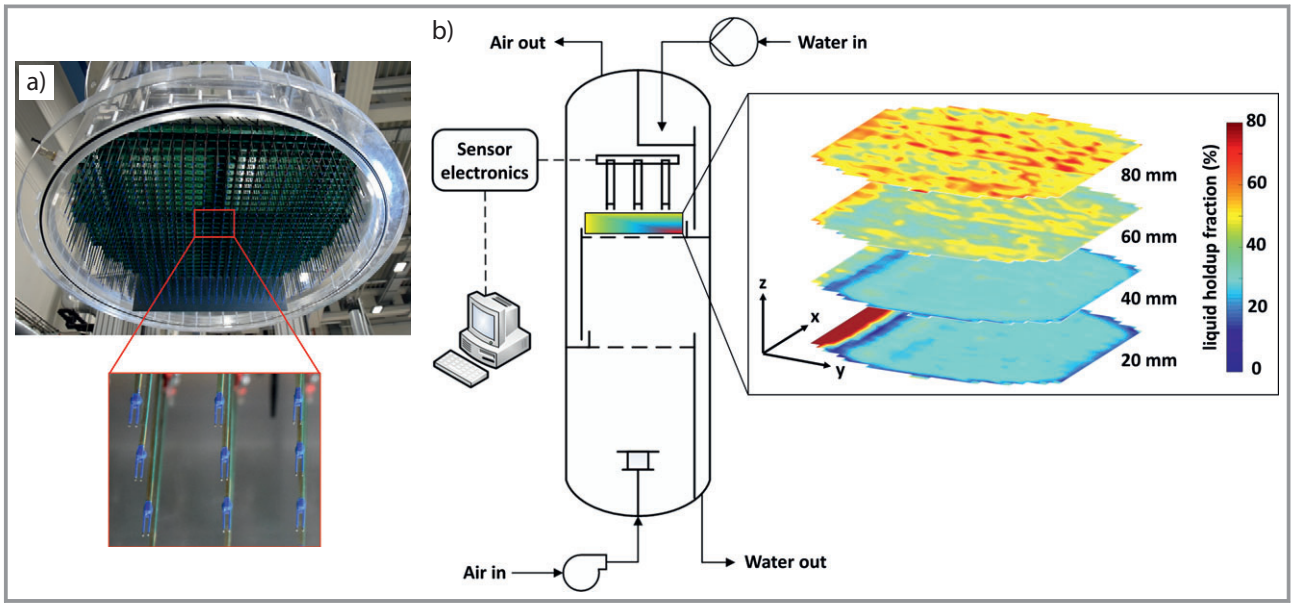

Figure 9. a) Multi-probe flow sensor for column trays. b) 3D liquid holdup distribution for an air-water column mock-up with sieve trays.

allows quantifying the average holdup and clear liquid height accurately. The sensor further permits identifying the liquid flow profiles (i.e., residence time distribution) on the tray via salt tracer studies.

3.4 Investigation of Two-Phase Flow in Feed Pipes (Helmholtz-Zentrum Dresden-Rossendorf)

Feeding distillation columns with a two-phase mixture may lead to heavy droplet entrainment in the column, which is highly detrimental to separation efficiency. The selection of proper inlet devices that control the flow and capture droplets requires knowledge of the flow conditions upstream. Short pipe lengths, complex pipe routing as well as varying operating conditions and fluid properties encountered in feed pipes hinder reliable prediction of the flow morphology and demand validated novel modelling approaches, such as CFD simulations or reduced order models. High-resolution flow imaging in complex feed pipes has been achieved with wire-mesh sensors (Fig. 10a). With that, 2D cross-sectional images of the phase distribution can be obtained at sampling rates up to 10 kHz. Analysis and visualization techniques are used to determine local flow parameters such as

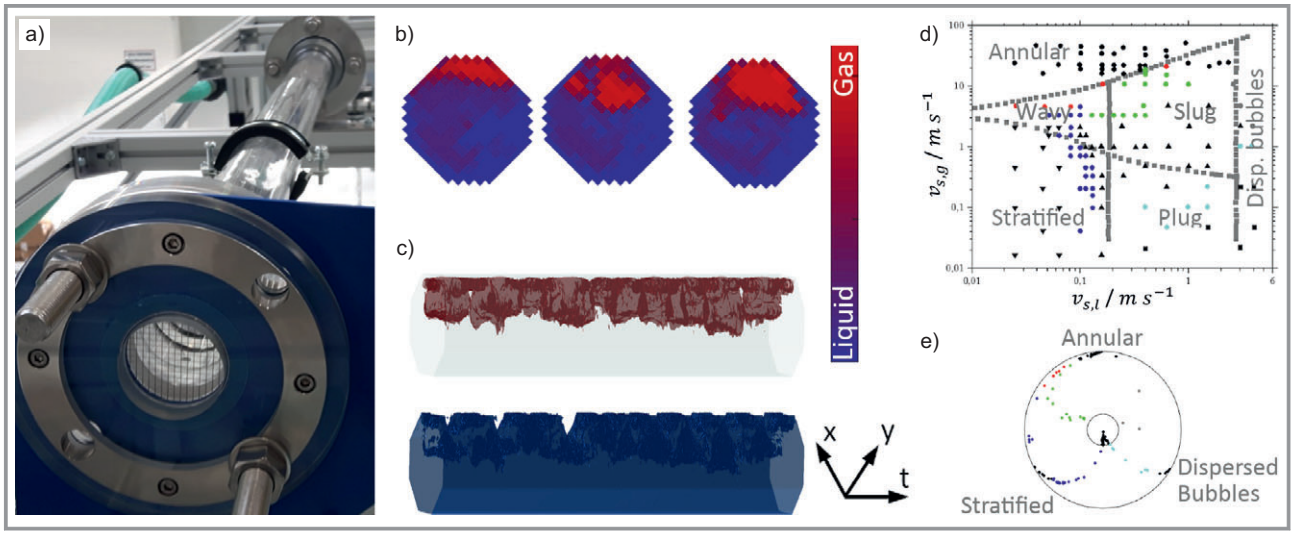

Figure 10. a) DN 50 feed pipe with wire-mesh sensors. b) Measured cross-sectional and axial phase distributions. c) Corresponding pseudo-3D representation. d) Flow morphology prediction by a conventional flow map and e) a novel classification method.

interfacial area, wetted wall fraction or power spectra. Figs. 10b and 10c show exemplarily results for the evolving flow in a feed pipe configuration. Conventional classification tools, such as flow regime maps [23], were tested against the encountered morphologies. The main flow regimes, that is, stratified, annular, intermittent, and dispersed bubbly flow (black symbols in Fig. 10d), are properly predicted while transitional regimes (colored symbols in Fig. 10d) deviate from the map. For more complex pipe configurations the flow morphology becomes more versatile. Here, the flow takes various morphology types along the pipe that are contrary to the static flow regime prediction by a flow regime map. Therefore, we developed a fuzzy identification algorithm [24] to reliably assign the spatio-temporal phase distribution to certain flow morphologies. In this novel morphology classification, every flow pattern is expressed in terms of degrees of membership to the four main regimes and five transitional morphologies (Fig. 10e).

3.5 Liquid Flow Analysis with Collector Techniques (TU Munich)

For the characterization of the liquid flow and maldistribution within packed columns, liquid collectors are frequently used. This measuring device enables the detection of the actual liquid volume flow instead of providing only an indication of it. Its common usage is also based on the fact, that measuring with a liquid collector is technically quite easy and inexpensive in its realization. For getting the absolute volume flows, and therefore the extent of maldistribution within a packed column, liquid collectors are one of the most accurate measuring techniques. There are a few restrictions for operating collectors, e.g., they can be installed only at the column bottom. Hence, this generates the need of varying the packing height if the liquid distribution should be analyzed relating to the liquid run length in the packing. Furthermore, it is impossible to get conclusions on the actual local mass transfer with a liquid collector only. As a result, the liquid distribution and therefore the fluid dynamics in the column without conclusions on mass transfer are gained.

TU Munich is operating a packed column test rig with an industrial relevant diameter of 1.2 m using a liquid collector as shown in Fig. 11a. The collector itself consists of seven concentric rings, which provide an annular structure. Each ring, except the undivided innermost one, is divided into three equal-sized sections. In total, this leads to 19 collector segments. In the collector segments, gas chimneys are installed to guarantee a uniform distribution of the gas in the whole cross-section of the packing. To avoid any interference of the collector with the flow in the packing, the gas chimneys are distributed according to their fraction of the total cross-sectional area. The 1.2 m diameter column provides feasible packing heights of 1.0, 1.5, 2.5, and 3.0 m. With the test rig liquid loads of u_L = 0...80 $m^3m^{-2}h^{-1}$ and

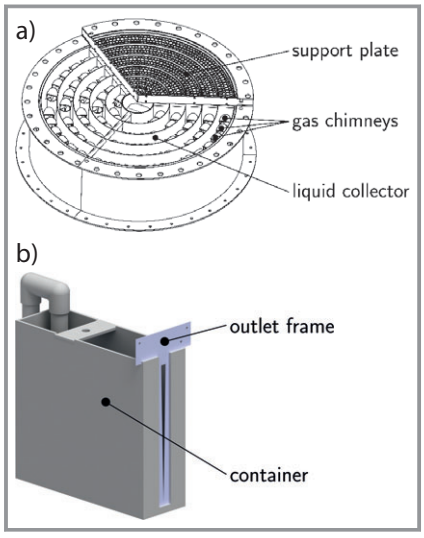

Figure 11. a) Liquid collector of the Ø 1.2 m packed column at TU Munich [25]. b) Measuring cell for determination of liquid flows [25].

gas loads of F = 0...4.7 $Pa^{0.5}$ are possible [25]. The packed column is operated with water and saturated air in a countercurrent flow. The powerful blower facilitates the exceeding of loading conditions and even flooding. This provides the possibility to analyze roughly the complete operating range of the packed column. Different packing types and sizes can be analyzed in the experimental apparatus. To gain insights into the flow condition during the experiments the column consists of several column sections made of transparent plastics. To characterize the liquid flow within the packing optimally, different liquid distributor types are employed, such as uniform and single point distributors. The liquid flow at the bottom of the column is collected in the 19 collector segments.

The measurement of the volume flow through each of the collector segments is realized with the measuring cells shown in Fig. 11b. One cell consists of a container and a V-shaped outlet frame. This frame ensures a constant low level measuring error even at very low volume flows. In each measuring cell the liquid level is detected. With a correlation between liquid level and outlet flow it is possible to measure the liquid level and calculate the volume flow of the liquid in one collector segment [25]. The test rig provides simultaneous measurement of the liquid volume flows through the 19 collector cells. This leads to a closure of the mass balance with only a slight error of ±5 % for 95 % and ±2 % for 63 % of more than 8500 recorded operating points [25]. The high degree of automation enables short measuring times and therefore the generation of a large database, which already allowed an improvement of modelling the liquid distribution [26]. Distribution data is available upon request.

3.6 Liquid Flow Analysis with Thermal Measurement Techniques (TU Munich)

To visualize the distribution of the liquid phase within a column, temperature measurements have been proven successful. The characterization of the phase distribution of water is based on the temperature profile within the column, which is induced by mass transfer processes. The partial evaporation of warm water causes a temperature decrease within the packing. This temperature decrease is relatively easy to detect. It is necessary that the temperature measurement within the column does not have any effect on the liquid and gas countercurrent flow. The main advantage of thermocouples is that they are only a few millimeters in size. Therefore, they are minimal-invasive for the fluid dynamic characteristic in the packing itself. Besides their small size, one of the main advantages of the temperature measurement with thermocouples is its indication of the local mass transfer within the packing. Thus, not only conclusions about the liquid flow, but also findings on the mass transfer, the actual interesting value itself, can be gained. Furthermore, it is possible to calculate the global separation efficiency of the packed column.

The Institute of Plant and Process Technology at TU Munich is operating a test rig with thermocouples. The measurement principle was originally used by Stichlmair [27] to determine the liquid flow on column trays. Besides trays, the method was also frequently applied with success to analyze the liquid distribution of the system water/air within packed columns [28]. The current test rig at TU Munich is a packed column operated with warm water and air in a countercurrent flow. At the column head, the water is fed on the packing, at the column bottom unsaturated air is injected. During an experiment, water is heated up by steam to about 43 °C before entering the packing at the column head. Different initial distribution types such as uniform or single point distributions are possible. The unsaturated air is warmed up because of the compression in the blower. To guarantee comparable initial conditions for each experiment, water is injected in the gas stream to cool down and humidify the airflow before it enters the packing evenly distributed. The column has an inner diameter of 0.634 m and a maximum packing height of 6.82 m. It consists of 11 transparent plastic column sections, each with 0.580 m in height, and 12 measurement flanges, each with 0.040 m in height, lying in-between. In each measurement flange 61 iron-constantan thermocouples, also known as thermocouples type L, are positioned in an equilateral triangle pattern. Thus, there are, in total, 732 thermocouples installed within the packed column. Each thermocouple is covered with a small piece of fabric, which gets soaked with water to ensure the temperature is taken only from the liquid and not the gas phase.

Fig. 12 shows a graphical visualization of the liquid distribution and with that the maldistribution in form of isotherms. In case of a perfectly distributed liquid phase, the isotherms appear in horizontal lines. The more the isotherms are curved the greater is the inequality of the liquid distribution and therefore the maldistribution. In Fig. 12 the unequal distribution and the effect of the wall flow is emphasized in the curved and therefore strongly non-horizontal isotherms.

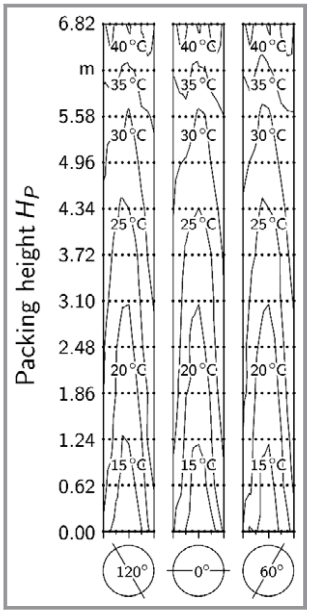

Figure 12. Temperature distribution in the Ø 0.634 m packed column at TU Munich. Hiflow® ring 25-7 plastic at a liquid load of $u_L = 5.8\ m^3m^{-2}h^{-1}$ and a gas load of $F = 1.2\ Pa^{0.5}$ with uniform initial liquid distribution. The dots (•) represent the positions of the thermocouples.

3.7 Analysis of Liquid Entrainment Assisted by Optical Imaging Techniques (TU Kaiserslautern)

Entrainment phase slip of liquid droplets above trays and packings lowers separation efficiency and constitutes a severe threat to column internals and connected downstream equipment. While previous research considers entrainment only as a consequence of changes in operation conditions or internal design, the application of an image-based in-line measurement technique [29] allows to understand local hydrodynamics and to make reliable predictions on integral changes. A new image-based telecentric probe developed by TU Kaiserslautern is used to analyze entrained liquid above trays and packings in two DN 450 columns (Fig. 13a). In dependence on internals, operation parameters and measurement position, droplet size distributions reach from the micrometer to the millimeter scale. For this purpose, an adjustment of the probe's measurement volume allows to prevent particle overlapping. Shadowgraphic images, rich in contrast, enable an analysis of the entrained droplets with respect to shape, size and velocity [30]. Experimental results reveal a strong correlation between droplet size and operation parameters but also on column and equipment design. The share of large droplets within a droplet size distribution increases (decreases) with advancing gas (liquid) loads when trays are operating in the froth regime. In contrast, the share of large droplets above

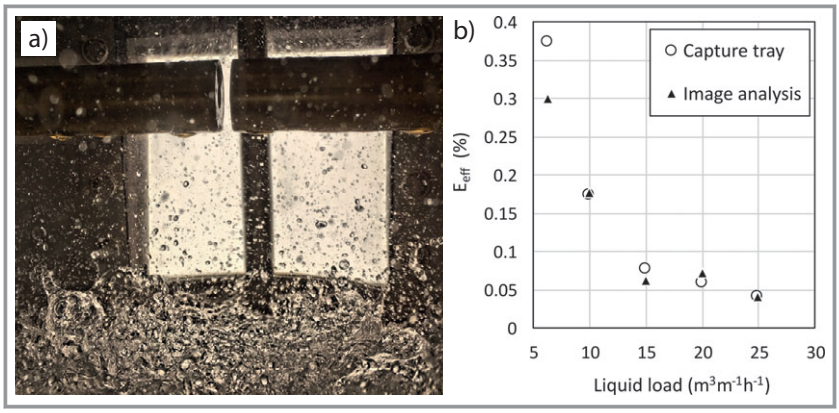

Figure 13. a) In-line probe with variable gap. b) Comparison of local and integral entrainment rate analysis [31].

packings increases with advancing gas and liquid loads. Furthermore, repositioning of the probe reveals a homogenous droplet size distribution across the column cross section with respect to sieve trays, while fixed valve trays and packings generate a higher share of larger droplets in the column center. As mentioned before, a precise image analysis also enables the estimation of the droplet velocity by a cross-correlation of two following images. Results reveal as expected higher velocities for smaller particles but also average particle velocities lower than the superficial gas velocity. In conclusion, the knowledge of particle size and velocity facilitates a determination of the local entrainment rate within the examined measurement volume. The consideration of multiple measurement positions enables an extrapolation of local entrainment rates to an integral value covering the whole column cross-section. A comparison between entrainment rates predicted by image analysis and those quantified by the conservative capture tray method shows good agreement (Fig. 13b) [31]. To sum up, in-line image analysis not only enables a better understanding of the hydrodynamics within columns by having a look into the process, but also to detect process changes earlier, to predict undesired operation conditions and to reduce costs by savings of material and labor due to substitution of conservative measurement methods.

4 Experimental Techniques for Evaporators and Condensers

4.1 Residence Time Measurement in Wiped Film Evaporators Using Near-Infrared Sensor Technology (TU Braunschweig, Hochschule Mannheim)

Due to their low liquid hold-up, good heat transfer characteristics and short residence times wiped film evaporators (WFE) are particularly suitable for the evaporation of thermally sensitive substances as well as fast chemical reactions. A proper assessment of the thermal stress exerted to a sensitive product as well as the estimation of conversion rates for chemical reactions builds on the reliable quantification of the residence time behavior of WFE under process conditions. For a tailored design and operation of WFE, knowledge on the influence of physical properties, equipment characteristics as well as operating conditions on residence time distributions (RTD) is essential. However, RTD are typically investigated under non-boiling conditions and atmospheric pressure [32], [33]. To reach a better insight on fluid dynamic effects during the evaporation within a wiped film apparatus two near-infrared (NIR) probes are used to investigate the residence time behavior under different evaporating conditions. A steam-heated stainless steel WFE with an evaporation area of 0.0643 m^2 and a typical throughput of 5 to 30 $kg\,h^{-1}$ is examined regarding its RTD characteristics. The feed flow consists of monoethyleneglycole with propylene carbonate as tracer. Measuring the tracer injection and outlet peaks allows a determination of residence time distributions for various operating conditions. An appropriate light excitation is implemented using LED light sources with a fixed wavelength of 1550 nm. The detector consists of broadband photodiodes and an amplifier board. Four fiber optic cables – two for each measuring position – with a diameter of 400 µm connect the light sources with the plant. The distance between each pair of NIR probes is adjustable to secure an equal voltage base line that guarantees linearity between the measuring signal and propylene carbonate concentration. The feed probe is installed directly after the manual tracer injection at the evaporator entrance (Fig. 14a). The bottom probe is situated after the outlet cone of the WFE corpus in a slightly inclined piping element to secure a sufficient wetting at the measurement point. Fig. 14b shows a typical diagram of both signals from the injection and outlet zone. Further data processing of the raw data sets is needed to extract characteristic values like mean residence time, the median value and variance.

4.2 Performance Investigation of Pillow-Plate Condensers (Paderborn University)

Advanced heat exchanger concepts are gaining more and more importance in view of rising energy prices and increasing environmental awareness. Among the most promising concepts are pillow-plate heat exchangers (PPHE), with their fully welded and hermetically sealed construction, high structural stability, compactness and lightweight. A unique pilot plant for studying condensation in PPHE has been built at Paderborn University and further

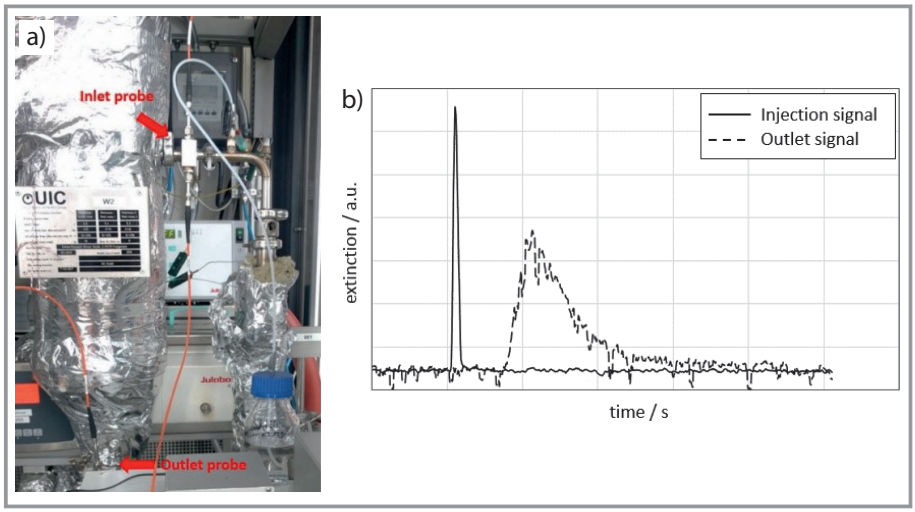

Figure 14. a) Implementation of NIR probes. b) NIR signal intensity at injection and outlet zone over time.

developed within the large consortium project InnovA^2 [34]. The main components of the condensation circuit are a reservoir, an evaporator, two pillow-plate condensers connected in series and containers collecting condensate (CCC, Fig. 15a). The evaporator is linked to the heating circuit, while the two pillow-plate condensers are linked to the cooling circuits. Vapor partly condenses in the upper partial condenser (PC). Full condensation of the remaining vapour takes place in in the total condenser (TC). Both condensers comprise three parallel, vertically oriented pillow-plates. The entering condensing steam flows from top to bottom in the outer channels between the pillow-plates, whereas the cooling medium flows countercurrently through the inner pillow-plate channels. The influence of inert components on the condensation behavior can be investigated, when an adjustable non-condensable gas stream (nitrogen) is continuously added to the steam line approaching the PC (Fig. 15a). After leaving the PC, the inert gas is removed at three different points to avoid accumulation.

The plant can be used to investigate the thermohydraulic condensation behavior and to determine overall heat transfer coefficients and pressure drop during the condensation of pure substances and binary mixtures, while three

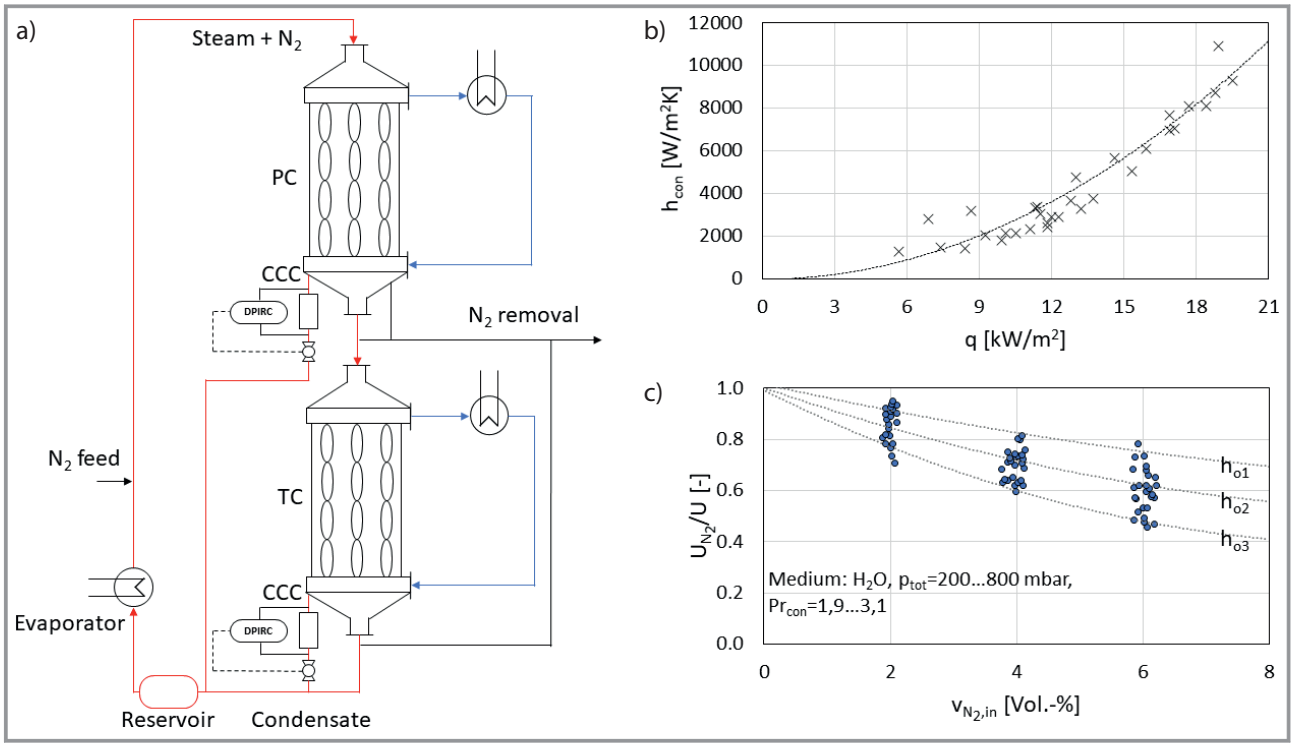

Figure 15. a) Simplified scheme of the condensation plant. b) Condensation heat transfer coefficients as a function of heat flux density: measurements for water at film Reynolds numbers between 10 and 60 (adapted from [34]). c) Ratio of overall heat transfer coefficients with (U_{N2}) and without (U) nitrogen evaluated for varied nitrogen volume fraction: single-phase heat transfer coefficients in outer channels $h_{o1}>h_{o2}>h_{o3}$ (adapted from [35]).

different methods are used to record the accumulated condensate mass flows. Pure substances as well as binary mixtures containing a non-condensable substance have been studied under different operating conditions [34, 35]. Using another experimental setup allowing heat transfer in the cooling channels to be determined [36], individual heat transfer coefficients in both, inner and outer channels, can be evaluated.

In the InnovA^2 project, several experimental studies on the condensation of water, iso-propanol and their mixtures with nitrogen have been carried out [34, 35]. In the experiments with pure water shown in Fig. 15b, the condensation heat transfer coefficients increased with rising heat flux density, but film Reynolds numbers remained low. This effect is attributed to the special design of the pillow-plates, which allows a better condensate drainage compared to normal vertical plates [34]. This results in a thinner condensate film thickness and therefore in a better heat transfer and condensation heat transfer coefficient due to a lower thermal resistance. Condensation performance worsens substantially when non-condensables are present (Fig. 15c) resulting in a significantly lower overall heat transfer coefficient [35]. This effect can be explained by diffusional effects in a boundary layer built up by the non-condensable component at the vapor-liquid interface.

Despite successful accomplishment of the measurements within InnovA^2, further investigations of condensation behavior are required. Such investigations are to be carried out in the context of the recently started collaborative project funded by the Federal Ministry for Economic Affairs and Energy, in which Paderborn University works together with partners from Kassel, Braunschweig and Munich. The pilot plant is now being used to investigate systems complementary to those from InnovA^2. Among others, experiments with binary condensable mixtures will be carried out and further measurements of systems containing inert components are foreseen. The new project will provide sufficient and reliable process data necessary for the understanding of complex condensation process in pillow-plate heat exchangers.

4.3 Assessment of Condenser Performance Based on Temperature Profile Measurements (TU Braunschweig)

Knowledge on internal temperature profiles in reactors, fluid separation columns or heat exchangers provides insights into the process and enables for a better assessment of process as well as equipment performance [37]. Tube side condensation in straight vertical tubes especially at vacuum conditions still presents a major source of uncertainty in equipment design and operation typically compensated by significant overdesign and increased operating costs. The temperature profile along the condensation path combined with reliable information on vapor-liquid equilibrium is a valuable indicator for the operating status as well as heat transfer performance of the equipment. Fiber optic temperature measurements have therefore been used to determine the axial temperature profile in a pilot scale condenser (Fig. 16a) at typical process conditions. A spatial resolution of about 1 cm at a frequency of 1 Hz was achieved, proving more than sufficient.

Condensation was performed in a five tube vertical condenser with tube geometry of $OD \times s \times L = 20 \times 2 \times 1800$ mm. Cooling water was used as service medium on the shell side with a constant inlet temperature of 60 °C. Fig. 16b presents the axial temperature profiles for the condensation of 1-hexanol vapor at a total pressure of 400 hPa with varied nitrogen flow. It is evident that without added nitrogen the condensation of the hexanol is completed after about 1 m tube length and the exit temperature pinches out with the cooling water inlet temperature. As nitrogen as non-condensing component is added condensation is not completed when bulk temperature has fallen below condensation temperature of pure hexanol. The product side temperature stays above 100 °C. An increased nitrogen flow is accompanied by an increased turbulence of the vapor side flow thus resulting in lower exit temperatures. This information may be used to design tailored tube geometries for effective condensation services as well as their quantitative performance assessment. Similar measurements at the evaporation side of a thermosiphon reboiler were less successful [38]. The

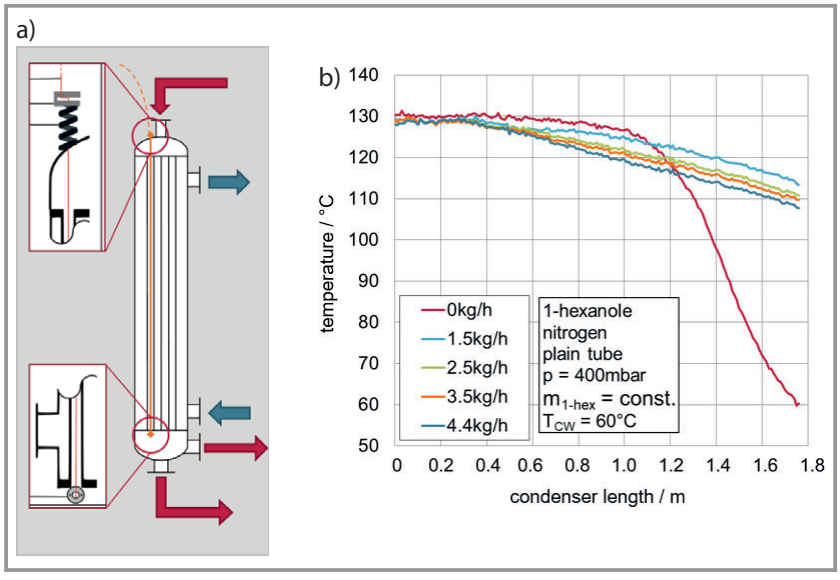

Figure 16. a) Sketch of the pilot scale condenser at TU Braunschweig that is equipped with fiber sensor technology. b) Axial bulk temperature profiles for the condensation of 1-hexanol inside vertical tubes with varied nitrogen content.

mechanical stress by the turbulent two-phase flow exerted a significantly stronger elongation of the glass fiber than the thermally induced expansion. So more research and development work is needed for this type of applications.

4.4 Resolving Local Fouling Kinetics Using Fiber Optic Temperature Measurements (TU Braunschweig)

The unwanted deposition of material on heat and/or mass transfer surfaces, referred to as fouling, presents a severe problem in many processes of the petrochemical, chemical, pharmaceutical and food producing industry, causing significant penalties in the energy efficiency of these processes. Its effect on the heat transfer performance of equipment is typically quantified via (thermal) fouling resistance. Although fouling kinetics shows different characteristic patterns and local variations, it is most frequently assessed with a single constant value for the fouling resistance giving an overall measure for the reduction of heat transfer due to the built-up of the fouling layer. However, a deeper understanding of the governing fouling mechanisms requires a quantitative spatial and temporal resolution of the fouling progress. Only this will allow tailoring equipment design and operating conditions for minimized fouling and maximum process energy efficiency.

Optical fiber technology allows for temperature measurements with high temporal and spatial resolution without or minimum interference with the actual process conditions. Depending on the respective technology, a spatial resolution of one to several centimeters at a data frequency of 1 Hz and higher is possible. With a given local heat flux, the local thermal fouling resistance may then be determined. A double pipe heat exchanger has been equipped with a fiber optic temperature measurement to determine the axial profile of the tube side wall temperature, see Fig. 18a [39]. The heat exchanger has dimensions $OD \times s \times L = 20 \times 2 \times 2000$ mm for the inner tube and $OD \times s \times L = 54 \times 2 \times 2000$ mm for the shell tube. It is operated in countercurrent mode with an aqueous $CaSO_4$ solution on the tube side and hot water as service medium on the shell side. Product inlet temperature is 42 °C and hot water inlet is 80 °C. Fig. 17 b depicts the evolvement of local fouling resistances at nine different positions. As expected, the fouling build-up starts from the hot end of the tube. Characteristic for crystallization fouling, an undershoot with negative values of the thermal fouling resistance can be seen in the initial phase, which is attributed to roughness and constriction effects of the growing crystal fouling layer [40]. Based on an assessment of the influence of roughness and constriction on local heat transfer, the fouling resistances can be corrected in an additional step to yield positive values [41]. This information may now be used to develop a mechanistic model for fouling kinetics as a function of component system properties, fluid dynamic conditions and equipment characteristics. Ultimately, this will allow for an improved design and operation of fouling-prone heat exchangers for increased process energy efficiency.

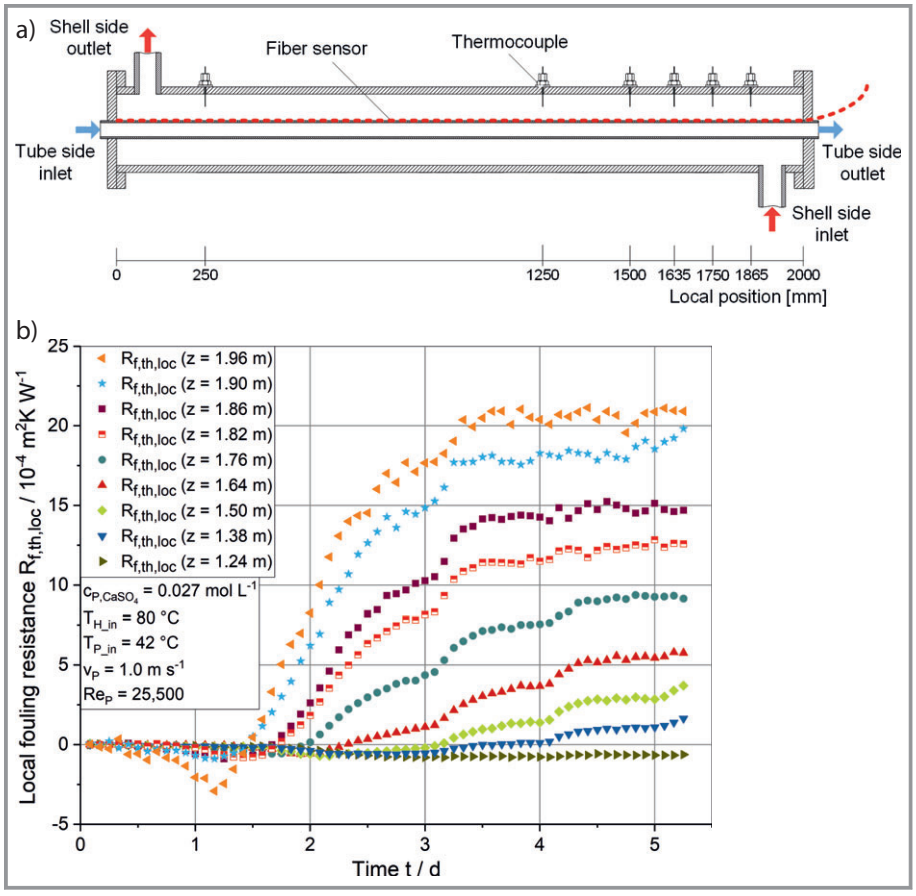

Figure 17. a) A double pipe heat exchanger has been equipped with a fiber optic temperature measurement to determine the axial profile of the tube side wall temperature, see Fig. 17a [39]. b) Local fouling resistances over time for calcium sulphate crystallization fouling in a double pipe heat exchanger.

5 Liquid-Liquid Separation Systems

5.1 Non-Invasive Measurement of Mass Transfer in Reactive Liquid-Liquid Systems (RWTH Aachen)

Reliable mass transfer data between two liquid phases is crucial for column modelling and design, but is often difficult to obtain in presence of a reaction. A tailor-made lab-scale reactor with a design according to Nitsch et al. [42] enables a decoupled investigation of reaction kinetics and mass transfer (Fig. 18a) [43]. As the cell material is Hastelloy C22, measurements with corrosive media, like inorganic acids at high temperatures up to 423 K and high pressures up to 15 MPa are possible. The cell is equipped with two independent stirrers for the convection of both liquid phases and glass internals to provide stable flow conditions. The rotational speed of the stirrers is adjusted so that the Reynolds number of both phases match. All biphasic experiments are thereby carried out with a stable phase boundary, which can be visually controlled through two sapphire glass windows. This allows a separate determination of the mass transfer kinetics and the phase boundary, since the latter can be calculated from the diameter of the cell. Subsequent biphasic reaction experiments follow the same procedure in presence of the catalyst. As the mass transfer was previously determined, direct conclusions on the reaction kinetics can be drawn from the results. Inline concentration measurements are performed by an FTIR-spectrometer equipped with a fiber-optic IN350-T silicon ATR-probe (Bruker Optik GmbH, Ettlingen, Germany) and a Raman spectrometer equipped with a fiber-optic short focus immersion sapphire probe (Kaiser Optical Systems, Ann Arbor, MI, USA). Compared to offline-analytics, it is beneficial that there is no need for sampling that disrupt the system or might be unstable. As the measurements are made in short intervals, nearly continuous concentration profiles are obtained and the partition of a transition component can be observed. Fig. 18b shows the molar concentrations of 5-hydroxymethylfurfural (5-HMF) over time for a mass transfer experiment in the two-phase system 2-methyltetrahydrofuran (2-MTHF)/water as an exemplary case. Using the mass transfer coefficient as a fitting parameter, a rate model describes the measured values accurately. The detailed description of 5-HMF mass transfer was included in a reaction kinetic model for the dehydration of 5-HMF from fructose. The resulting model allows an accurate prediction of the biphasic reaction kinetics and was integrated in the model-based design of a tailored reactor unit [43].

5.2 Optical In-Line Particle Analysis for Liquid-Liquid Systems (TU Kaiserslautern)

Image analysis of droplets in liquids is done at TU Kaiserslautern with a telecentric probe. It bases on a shadowgraphic technique [29] where independent from position the true droplet size is detected and thus a calibration is not required. The first variant of the shadowgraphic probe consists of two invasive tubes with glass windows in the front. Both tubes form a measurement volume where the particles are captured. One tube contains the illumination (LED) unit generating a parallel light bundle and the other side is the camera unit with a telecentric lens. Hence, the camera system generates high contrast images that can be easily analyzed by image processing. Additionally, the telecentric lens provides an optical imaging where the size of the particles does not depend on the position or distance in the field of view, resulting in a real measurement volume instead of a small focal plane. Measurement flanges for various kinds of apparatuses are used to integrate the measurement system (Fig. 19a). Starting from droplets an extension was to ellipsoid bubbles

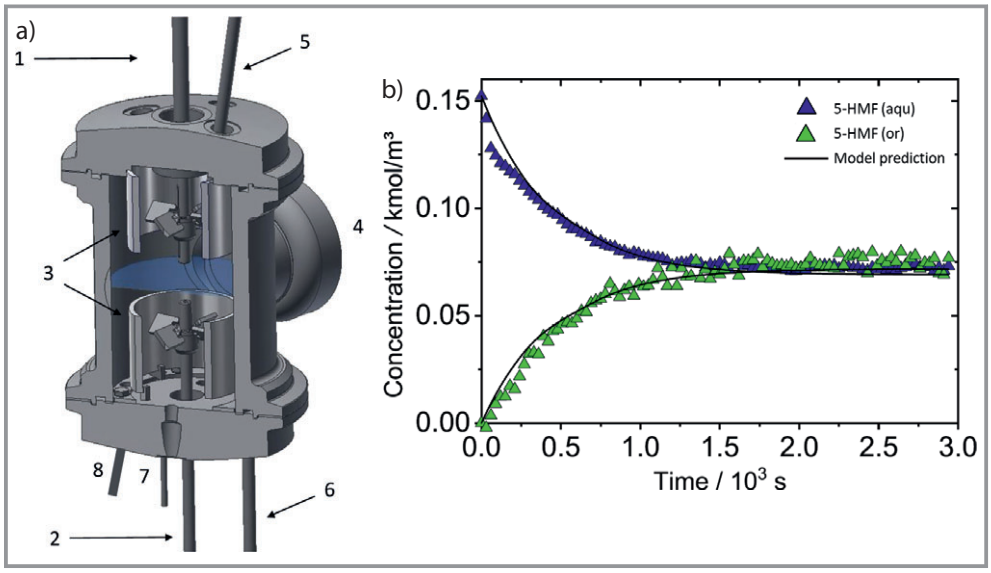

Figure 18. a) Hastelloy reactor for mass transfer and kinetic experiments: 1,2: stirrer for heavy and light phase, 3: flow internals, 4: glass window, 5,6: Raman and FT-IR probes, 7: sampling port, 8: inlet for HPLC pump. b) Concentration profile for a mass transfer experiment of 5-HMF in the two-phase system 2-MTHF/water. [43].

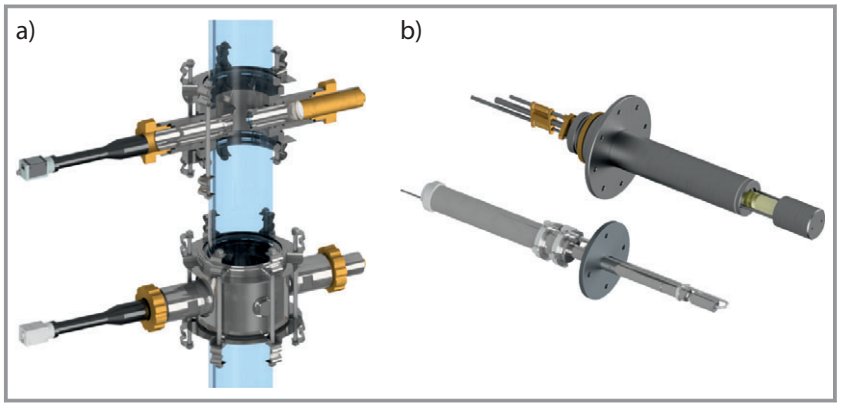

Figure 19. a) Installation view of the telecentric probe. b) CAD drawing of a single-sided probe.

with different probe size according to apparatus (DN 100 to DN 450) and pipe (DN 25) dimensions. In addition to the conventional image processing procedures, like binarization, segmentation and detection, a convolutional neural network has been trained for droplet analysis. Computer generated images with known droplet size have been used to train the algorithm. The neural network improves segmentation at higher phase fractions and has been tested up to phase fractions of 25 vol % [30] To simplify the integration of the measurement system and therefore to get access to industrial scale, a one-sided probe has been developed retaining the full functionality of the telecentric shadowgraphic measurement principle. The probe is fully adjustable, regarding measurement volume and position in the apparatus and is integrated via a DN 80 flange. In order to decrease invasivity, a more compact probe for a DN 50 flange is being developed (Fig. 19b).

The probe is easily applicable for extraction columns, stirred vessels and phase separators to control entrainment or validate simulations. The later relies on population balances in a user-friendly GUI as depicted in Fig. 20, here in a start-up period. One can select process and simulation parameters and below turn up online images of the telecentic probe. On the right-hand side in the top is the simulation (white line) of the particle diameter versus conductivity measurement (green line). The diagram below shows holdup simulation (blue line) versus measurement (brown line) and a prediction horizon (white line). In both diagrams the simulated predictions are given by dottet lines. In the bottom there is holdup (white line) and particle diameter (red line) and the other side the actual droplet size distribution [44]. In conclusion, this measurement technique offers broad application, such as in rectification columns (sieve, trays and packings in section 2.7), extraction equipment (mixer-settlers, columns, pumps), crystallization and has also been successfully tested in solid-gas-liquid systems. It is a powerful tool when it comes to the inline determination of particle characteristics, even in an industrial environment.

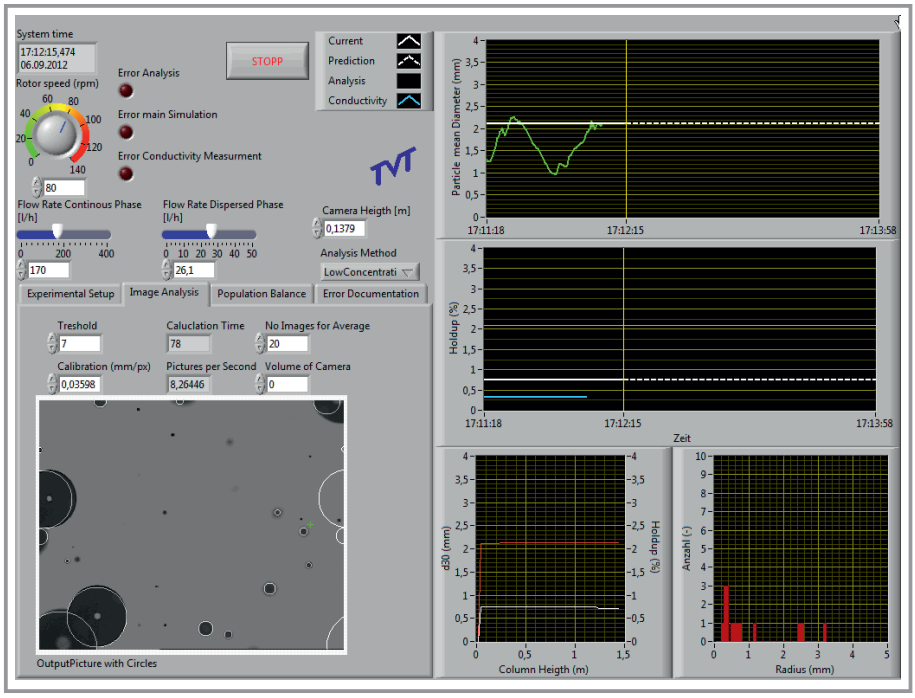

Figure 20. Droplet distribution on-line monitoring via LabVIEW.

5.3 Analysis of Extraction and Crystallization Processes with Raman Spectroscopy Techniques (TU Bergakademie Freiberg)

Still today, the projection of apparatuses for liquid-liquid extraction and for crystallization is largely based on experimental experience. Often, several upscaling steps are required for a reliable provision of an industrial-scale process that meets the desired specifications. Here the application of in situ Raman spectroscopy can help accessing in real-time the efficiency of separation stages, not only in single-phase systems, but also in multi-phase systems. As electronic compounds, such as lasers, spectrometers and computers have become smaller, more reliable, more robust and better, Raman spectroscopy is well suited for permanent process monitoring, also under harsh conditions in industrial environments.

Fig. 21b shows a Raman probe developed for the in situ monitoring of the supercritical carbon dioxide (CO_2) extraction of hops. The probe resists pressures up to 600 bar and can be directly screwed into a steel pipe via an NPT thread. Other connectors, such as flanges, or Swagelok fittings have been realized too. With a temporal resolution of up to 1 Hz (faster is possible) the fraction of alpha-acid in the extract stream was monitored, as it is shown for a reduced sampling rate in Fig. 21b. As the properties of natural products vary depending on the harvesting period, the growing region, the storage conditions and many more, the extraction of each batch is more or less specific. Based on the in situ measurements the operator of the extraction plant can optimize the extraction process (duration) to the extraction yield [45].

The Raman spectra of many compounds depend on their chemical environment. Thus, the position, the widths or the shape of certain Raman peaks provides information about the chemical environment the compound is dissolved in. With respect to liquid-liquid systems, where one compounds is partitioned over two liquid phases, the two liquid phases are different with respect to their composition and thus feature different chemical environments. Thus, one can deduce the partition of the compounds over the phases from the Raman spectrum of the multi-phase mixture. Consequently, mass transfer processes are accessible in situ and even in multi-phase liquid-liquid systems.

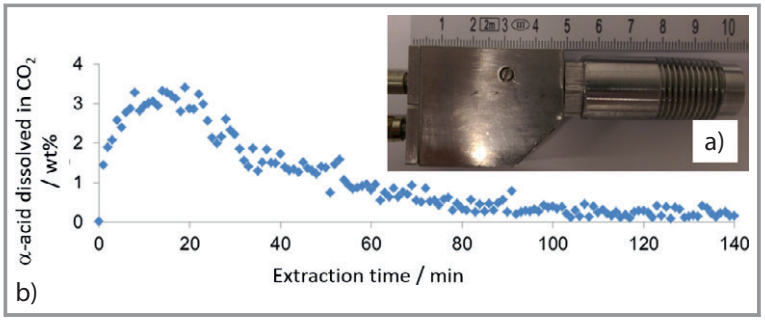

Figure 21. a) Photograph of a Raman probe with NPT thread for pressures up to 600 bar. b) Temporal evolution of the alpha-acid weight fraction in the extract stream during the supercritical CO_2 extraction of hops.

What is reported above for the partition of one compound over two liquid phases is also true for the partition of one compound over a liquid and a solid phase and thus is relevant for crystallization. Figure 22a shows Raman spectra of a drug acquired during the crystallization of the drug from a solution. Here the peak of the drug in its crystalline solid form is left-shifted with respect to the drug in the dissolved state. Therefore, from the growth of the crystalline drug peak and the shrinkage of the dissolved drug peak one can extract information about the growth of the solid phase or the conversion of the dissolved drug into the solid drug. Fig. 22b shows the kinetics of the growth and the shrinkage of both peaks. With respect to the three examples provided above, the successful realization of the Raman measurements depends to a certain extend on the specific design of the Raman probe and on the processing of the obtained raw Raman spectra, which are main competences of the research team of Andreas Braeuer at TU Bergakademie Freiberg [46, 47].

5.4 Characterization of Liquid-Liquid Phase Separation by Ultrasound Scanning Technology (Bayer AG)

Bayer AG develops a new experimental setup and procedure combining ultrasound scanning technology with standard settling tests for the characterization of phase separation behavior of liquid-liquid systems. For the validation of both, experimental setup and method, two standard organic/aqueous test systems (cyclohexanone/water and butylacetate/water) as well as one technical system, where conventional visual methods cannot be applied, were investigated. The results show that this method allows the determination of the required phase separation parameters for the design of gravity settlers for opaque systems, using standard scale-up procedures as well as the complete automatization of the measuring technique.

The characterization of phase separation of liquid-liquid dispersions is of major importance for the design of industrial equipment (batch and conti operated equipment as liquid decanters, mixer-settlers, extraction columns). Unfortunately, modelling is up to now not able to cope with the prediction of the settling behavior for multicomponent and technical liquid-liquid mixtures. Therefore, experimentation is a must in order to obtain the required phase separation parameters. Bayer AG uses standardized batch-settling trials based on the experimental setup and procedure developed by Henschke [48] to obtain the necessary data for the design of gravity settlers, based on sedimentation and coalescence curves. However, over the last years, more and more cases of

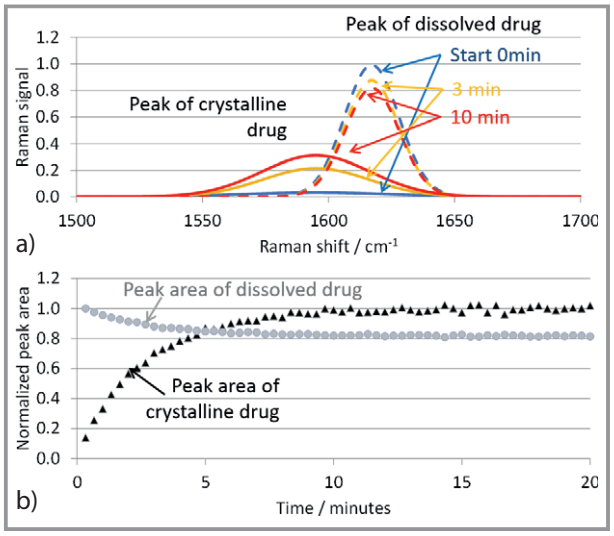

Figure 22. a) Raman spectra of a pharmaceutical drug at different times during batch crystallization. b) Evolution of the growth or the shrinkage of the crystalline (solid) and dissolved drug peak intensities.

"dark-dark", opaque or very turbid systems have been noted. It is therefore required to develop an alternative standardized non-visual method – not only to determine the phase separation times, but also to separately define the sedimentation and coalescence curves and identifying the "dense packed zone" for further determination of the drop size. Based on the difference in physical properties of the two liquid phases (e.g., density, viscosity, speed of sound) an alternative measuring technology can be used to overcome the limitations of visual methods. Based on the previous work developed by Pfennig et al. [49] and Shaw et al. [50], Bayer AG develops a new experimental setup and procedure combining ultrasound scanning technology with the standard settling cell developed by Henschke [48]. This method allows the determination of the required phase separation parameters for non-transparent systems, using standard scale-up procedures as well as the complete automatization of the measuring technique.

Fig. 23a shows part of the experimental setup that consists of the ultrasound phased-array sensors (developed in collaboration with University of Alberta and the company Action-NDT) attached to the settling cell, the high-speed acquisition unit Focus PX and the associated software Focus PC (both from Olympus). Fig. 23b shows a comparison of experimental sedimentation and coalescence curves determined by visual and ultrasound methods (average values) for the system cyclohexanone/water (Vo/Vw = 2/1, n = 250 min^{-1}, T = 20 °C, f = 1 Hz). The diagram shows a good match between the visually recorded coalescence and sedimentation curve and those recorded with the applied ultrasound scanning technology.

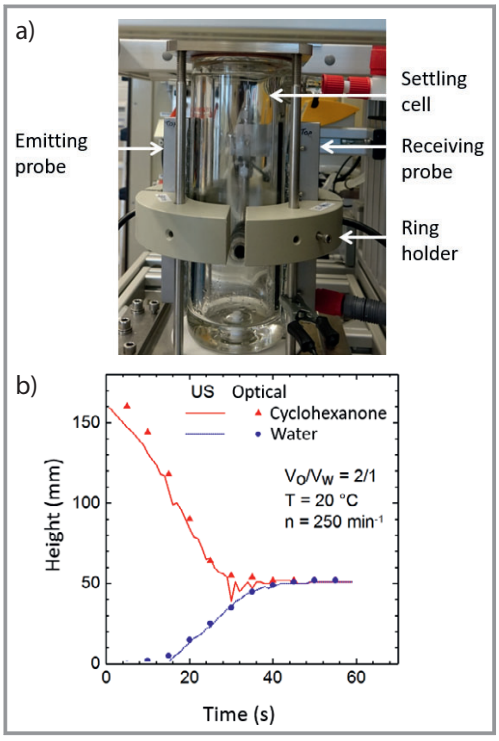

Figure 23. a) Experimental setup showing ultrasound probes attached to the settling cell. b) Example of comparison of sedimentation and coalescence curves obtained by visual method vs. ultrasound scanning technology (US) for the system cyclohexanone + water with volumetric phase ratio organic to water Vo/Vw = 2, rotational speed n = 250 min^{-1}, temperature T = 20 °C, and frequency f = 1 Hz.

6 Intensified Separation Technologies

6.1 Investigation of Two-Phase Flow and Mass Transfer in Rotating Equipment (TU Dortmund University, Helmholtz-Zentrum Dresden-Rossendorf)

While the exploitation of centrifugal fields for the intensification of gas-liquid contacting has been under consideration for more than 60 years, rotating packed beds (RPB) and other so-called high-gravity equipment received a significant increase in interest over the last 10 to 20 years, with several industrial applications, primarily in Asia [51]. Despite a rich literature on experimental investigations for various applications, experimental insight into the hydrodynamic conditions and mass transfer inside of an RPB and especially inside of the annular-shaped packing is severely limited. However, such insight is of special importance for reliable modelling and design of an RPB, because unlike static packed columns, the cross-sectional area as well as the liquid and gas velocities cannot be considered constant with the radial depth of the packing, in which they are counter-currently contacted. Therefore, innovative and

potentially tailored measurement techniques need to be developed to generate the necessary insight.

RPBs rely on a motor-accelerated rotor that is rotating at rotational speeds between 300 and 1200 rpm, which corresponds to accelerations of 10 to 250 times the gravitational acceleration at the inner diameter of the equipment. To quantify the local liquid holdup within the rotating internals researchers of TU Dortmund University and Helmholtz-Zentrum Dresden-Rossendorf applied gamma-ray computed tomography (CT). With its high-energy isotopic Cs-137 (662 keV) source it achieves good penetration of the RPB materials and furthermore gives time-averaged angle-resolved CT scans. The CT system can sample projections very rapidly at 22 kHz and therefore has the ability to create sharp reconstructions even at high rotational speeds of 1200 rpm. A Hall effect sensor was used for the synchronization between the RPB and the CT systems. Fig. 24a illustrates the setup for the gamma-ray tomography while Fig. 24b shows exemplarily the liquid holdup for a rotor of 146 mm inner diameter, 500 mm outer diameter and 10 mm axial height rotating at 1200 rpm. Based on the scans, the distribution of the liquid hold-up along the radius can be analysed and the influence of rotational speed, as well as other factors, such as the liquid and gas flow rate, can be evaluated (Fig. 24c). The generated data allows for the identification of operational limitations as well as the reasons for and degrees of maldistribution, as further described in an article of Groß et al. [52]. This information is essential for designing and optimizing the structure of the packing in the RPB.

The evaluation of concentration profiles along the radial length of the packing would be of highest value for analysing the mass transfer, but even temperature measurements in the rotating packing are challenging. In order to enable such measurements, a tailored telemetry setup for distillation in an RPB was developed by researchers of TU Dortmund and Caemax imc group. Wireless transmission of signals allows monitoring the temperature profile in the rotor for different rotational speeds, vapor-liquid flow rates and packing types. With a 16-bit resolution of the transmitter and the receiver, a temperature change of up to 0.0025 K can be detected with a sampling rate of 0.2 ms. For the current setup, Pt1000 temperature sensors with an accuracy class A ($0.15\,°C + 0.002 \cdot |T|$) were installed. Details of the experimental setup for total-reflux distillation in a single-stage RPB are described in a recent article by Qammar et al. [53].

The data on temperature change along the radial packing depth helps to resolve the local mass transfer inside of the rotating packing, which is an important prerequisite for the development of scale-up and design rules for this high-gravity equipment. A sketch of the sensor installation in the rotor is provided in Fig. 24d, while the illustration of the rotor plate provided in Fig. 24e indicates the position of the sensors implemented along the radial packing depth. Furthermore, the measured temperature data for the distillation of an ethanol-water mixture at atmospheric pressure is shown in Fig. 24f for a rotor with an inner diameter of 146 mm, an outer diameter of 600 mm and an axial height of 10 mm and an implemented packing with inner and outer diameter of 148 and 560 mm [53].

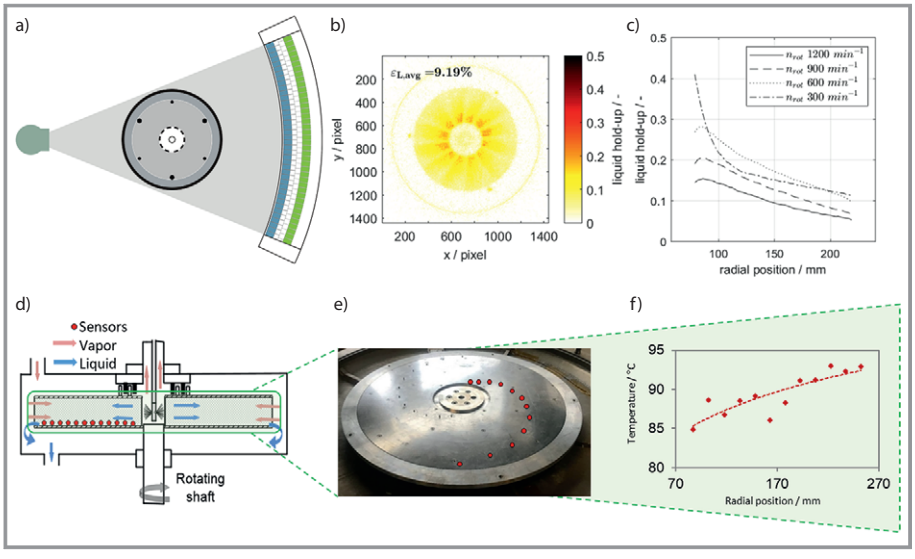

Figure 24. a) Gamma-ray tomography setup. b) Cross-sectional liquid distribution measured with gamma ray CT. c) Comparison of radial liquid hold-up for 1200 to 600 rpm rotor speed at $\dot{V}_G$ = 60 m^3h^{-1} and 300 rpm at $\dot{V}_G$ = 45 m^3h^{-1} and $\dot{V}_L$ = 0.378 m^3h^{-1} (multi-point distributor) for the full foam packing. d) Schematic drawing of RPB. e) Position of the temperature sensors for temperature telemetry along the radial packing depth of the rotor. f) Measured temperature profile at 600 rpm in the ZickZack packing.

7 Summary

The compilation in this article demonstrates the excellent capabilities of different academic and industrial research institutions to contribute to an advanced experimental analysis, understanding, and modelling of systems and components of industrial separation technology. Most notably, all available experimental facilities are equipped with state-of-the-art measurement techniques for phase distributions, gas and liquid flow, as well as heat flux and mass transfer analysis. This comprises modern laser-based flow measurement and process analytical tools, computed tomography scanners and distributed sensor systems. A number of facilities can be operated with organic

fluids, which is a critical concern when translating experimental findings to industrial separation problems. Another key aspect is the scale-bridging concepts of such experimental technologies, which is required as industrial separation is inherently a multiscale problem. Hence, analysis and model development do not only require multiscale simulation approaches but also true multiscale experiments and measurement technologies. It will be an important future concern to make synergetic use of these technologies to answer open questions of industrial separation systems which may come from new technologies and changing societal and economic boundary conditions.

References

[1] *Distillation: Fundamentals and Principles*, 1st ed. (Eds: A. Gorak, E. Sorensen), Academic Press, Cambridge, MA **2014**.

[2] J. Mackowiak, *Fluid Dynamics of Packed Columns, Principles of the Fluid Dynamic Design of Columns for Gas/Liquid and Liquid/Liquid Systems*, Springer, Heidelberg **2010**.

[3] M. Pilling, D. Summers, M. Fischer, in *Distillation and Absorption 2006* (Ed: E. Sørensen), IChemE, London **2006**, 317-326.

[4] G. E. Cortes Garcia, J. v. d. Schaaf, A. A. Kiss, *J. Chem. Technol. Biotechnol.* **2017**, *92 (6)*, 1136–1156.

[5] M. Schubert, A. Bieberle, F. Barthel, S. Boden, U. Hampel, *Chem. Ing.-Tech.* **2011**, *83 (7)*, 979–991.

[6] S. J. Gerke, J.-U. Repke, *Chem. Eng. Res. Des.* **2019**, *147*, 634–643.

[7] V. Kapoustina, J. Guffart, A. Hien, J. Strischakov, I. Medina, M. Rädle, J.-U. Repke, *Chem. Eng. Res. Des.* **2019**, *146*, 352–362.

[8] J.-U. Repke, M. Kohrt, G. Wozny, *Chem. Ing. Tech.* **2011**, *83 (7)*, 1107–1114.

[9] H. Leuner, M. Hapke, J. Sacher, M. Grünewald, J.-U. Repke, *Chem. Ing. Tech.* **2019**, *91 (1–2)*, 110–117.

[10] D. Toye, M. Crine, P. Marchot, *Meas. Sci. Technol.* **2005**, *16 (11)*, 2213–2220.

[11] A. Janzen, J. Steube, S. Aferka, E. Y. Kenig, M. Crine, P. Marchot, D. Toye, *Chem. Eng. Sci.* **2013**, *102*, 451–460.

[12] L. Bolenz, F. Fischer, D. Toye, E. Y. Kenig, *Chem. Ing. Tech.* **2019**, *91 (12)*, 1892–1896.

[13] S. Schug, W. Arlt, *Chem. Eng. Technol.* **2016**, *39 (8)*, 1561–1569.

[14] T. Linder, P. Leicht, M. Sommerschuh, A. Bösmann, P. Preuster, K. Müller, W. Arlt, P. Wasserscheid, M. Thommes, *Fluiddynamische Untersuchungen mittels Computertomographie*, Jahrestreffen der ProcessNet-Fachgruppen Fluidverfahrenstechnik, Adsorption und Extraktion, Berchtesgaden, Germany, February **2020**.

[15] F. Fischer, U. Hampel, *Nucl. Eng. Des.* **2010**, *240*, 2254–2259.

[16] J. Sohr, M. Bieberle, G. R. George, S. Flechsig, E. Y. Kenig, M. Schubert, U. Hampel, *Chem. Eng. Res. Des.* **2019**, *147*, 676–688.

[17] N. Hüser, E. Y. Kenig, *Chem. Eng. Trans.* **2014**, *39*, 1417–1422.

[18] N. Hüser, M. Yazgi, T. Hugen, T. Rietfort, E. Y. Kenig, *AIChE J.* **2018**, *64*, 4053–4065.

[19] R. Hoffmann, T. Kögl, *Flow Meas. Instrum.* **2017**, *53*, 147–153.

[20] M. Grünewald, J. Brinkmann, M. Hapke, F. van Holt, *Chem. Eng. Trans.* **2018**, *69*, 103–108.

[21] V. Vishwakarma, M. Schubert, U. Hampel, *Chem. Eng. Sci.* **2018**, *185*, 182–208.

[22] V. Vishwakarma, E. Schleicher, M. Schubert, M. Tschofen, M. Löschau, *DE Patent 10 2018 124 501.7*, **2018**.

[23] G. W. Govier, K. Aziz, *The Flow of Complex Mixtures in Pipes*, Van Nostrand Reinhold Ltd., London **1972**, 503–616.

[24] P. Wiedemann, A. Döß, E. Schleicher, U. Hampel, *Int. J. Multiphase Flow* **2019**, *117*, 153–162.

[25] F. Hanusch, S. Rehfeldt, H. Klein, *Chem. Eng. Technol.* **2018**, *41 (11)*, 2241–2249.

[26] F. Hanusch, R. Kender, V. Engel, S. Rehfeldt, H. Klein, *AIChE J.* **2019**, *65*, e16598.

[27] J. Stichlmair, *Untersuchungen zum stationären und dynamischen Verhalten einer adiabat betriebenen Absorptionskolonne*, Dissertation, Technische Universität München **1971**.

[28] F. Kammermaier, *Neuartige Einbauten zur Unterdrückung der Maldistribution in Packungskolonnen*, Fortschritt-Berichte VDI Reihe 3, Vol. 892, VDI Verlag, Düsseldorf **2008**.

[29] M. Lichti, H.-J. Bart, *ChemBioEng Rev.* **2018**, *5*, 79–89.

[30] J. Schäfer, P. Schmitt, M. W. Hlawitschka, H.-J. Bart, *Chem. Ing. Tech.* **2019**, *91 (11)*, 1688–1695.

[31] J. Schulz, K. Schäfer, H.-J. Bart, *Chem. Ing. Tech.* **2020**, *92 (3)*, 256–265.

[32] P. M. Schweizer, F. Widmer, *Verfahrenstechnik* **1981**, *15*, 29–33.

[33] J. Cvengroš, Š. Pollák, M. Micov, J. Lutišan, Film wiping in the molecular evaporator, *Chem. Eng. J.* **2001**, *81 (1–3)*, 9–14.

[34] J. M. Tran, M. Piper, E. Y. Kenig, *Experimentelle Studie zu der Filmkondensation von Wasserdampf im welligen Kanal zwischen Thermoblechen*, Jahrestreffen der Fachgemeinschaft Wärme- und Stoffübertragung, Baden-Baden, Germany, März **2013**.

[35] J. M. Tran, M. Piper, E. Y. Kenig, *Modelling of heat transfer and fluid dynamics in pillow-plate condensers based on experimental investigations*, ACHEMA 2015, Frankfurt am Main, Germany, June **2015**.

[36] J. M. Tran, S. Sommerfeld, M. Piper, E. Y. Kenig, *Chem. Eng. Res. Des.* **2015**, *99*, 67–74.

[37] C. Stegehake, M. Grünewald, H.-W. Zanthoff, C. Hecht, *Chem. Ing. Tech.* **2018**, *90 (5)*, 602–614.

[38] R. Goedecke, T. Sieger, P. Drögemüller, D. Samiek, S. Scholl, *Einsatz von faseroptischer Temperaturmessung in einem Laborverdampfer und -kondensator*, Jahrestreffen der ProcessNet-Fachgruppen Fluidverfahrenstechnik, March 15–17, Garmisch-Partenkirchen **2016**.

[39] F. Schlüter, L. Schnöing, H. Zettler, W. Augustin, S. Scholl, *Heat Transf. Eng.* **2020**, *41*, 149–159.

[40] F. Albert, W. Augustin, S. Scholl, Roughness and constriction effects in crystallization fouling, *Chem. Eng. Sci.* **2011**, *66*, 499–509.

[41] F. Schlüter, W. Augustin, S. Scholl, Introducing a holistic approach to model and link fouling resistances. Heat Mass Transf., submitted.

[42] W. Nitsch, *Faraday Discuss. Chem. Soc.* **1984**, *77*, 85–96.

[43] M. Aigner, D. Roth, J. Rußkamp, A. Jupke, *AIChE J.* **2020**, *66*, e16849.

[44] M. Mickler, H. Jildeh, H.-J. Bart, Online monitoring, simulation and prediction of multiphase flows, *Can. J. Chem. Eng.* **2014**, *92*, 307–317.

[45] J. J. Schuster, L. A. Bahr, L. Fehr, M. Tippelt, J. Schulmeyr, A. Wuzik, A. S. Braeuer, *J. Supercrit. Fluids* **2018**, *133*, 139–145.

[46] M. T. Gebrekidan, C. Knipfer, A. Braeuer, Vector casting for noise reduction, *J. Raman Spectrosc.* **2020**, *51 (4)*, 731–743.

[47] T. C. Klima, A. S. Braeuer, *Fuel* **2019**, *238*, 312–319.

[48] M. Henschke, *Dimensionierung liegender Flüssig-flüssig-Abscheider anhand diskontinuierlicher Absetzversuche*, Fortschritt-Berichte VDI, Reihe 3, Verfahrenstechnik, Nr. 379, VDI-Verlag, Düsseldorf **1995**.

[49] I. Aunyindee, A. Cano Castro, P. Chuttrakul, A. Pfennig, *Application of Ultrasonic Spectroscopy to Quantify Sedimentation of Polydisperse Emulsions*, in Book of Abstracts Minisymposium Verfah-

renstechnik – Leoben, Verlag der Montanuniversität Leoben, Leoben **2013**.
[50] M. Khammar, J. M. Shaw, *Rev. Sci. Instrum.* **2011**, *82*, 104902.
[51] K. Neumann, K. Gladyszewski, K. Groß, H. Qammar, D. Wenzel, A. Górak, M. Skiborowski, A guide on the industrial application of rotating packed beds, *Chem. Eng. Res. Des.* **2018**, *134*, 443–462.
[52] K. Groß, A. Bieberle, K. Gladyszewski, M. Schubert, U. Hampel, M. Skiborowski, A. Górak, *Chem. Ing. Tech.* **2019**, *91 (7)*, 1032–1040.
[53] H. Qammar, K. Gladyszewski, A. Górak, M. Skiborowski, *Chem. Ing. Tech.* **2019**, *91 (11)*, 1663–1673.

